

Defects chemistry in high-efficiency and stable perovskite solar cells

Cite as: J. Appl. Phys. 128, 060903 (2020); doi: 10.1063/5.0012384

Submitted: 30 April 2020 · Accepted: 28 July 2020 ·

Published Online: 11 August 2020



View Online



Export Citation



CrossMark

Yihua Chen  and Huanping Zhou^a 

AFFILIATIONS

Beijing Key Laboratory for Theory and Technology of Advanced Battery Materials, Key Laboratory of Polymer Chemistry and Physics of Ministry of Education, BIC-ESAT, Department of Materials Science and Engineering, College of Engineering, Peking University, Beijing 100871, China

Note: This paper is part of the special collection on Hybrid Organic-Inorganic Halide Perovskites

^a**Author to whom correspondence should be addressed:** happy_zhou@pku.edu.cn

ABSTRACT

It is the defects that determine the physicochemical properties and photoelectrical properties of the corresponding semiconductors. Controlling defects is essential to realize high-efficiency and stable solar cells, particularly in those based on hybrid halide perovskite materials. Here, we review the defect chemistry in perovskite absorbers, most of which take effects at grain boundaries and surfaces. These defects impact kinetics and/or thermodynamics during the courses of charge recombination, ion migration, and degradation in the corresponding devices, which inevitably influences their efficiency and stability. The effective suppression of harmful defects in perovskite photovoltaics not only reduces non-radiative recombination centers to improve the efficiency, but also retards their degradation under aging stresses to dramatically improve their long-term operational stability. Finally, the future challenges with regard to the in-depth understanding of defects formation, migration, and their passivation are presented, which shed light on realizing high-efficiency and stable perovskite optoelectronics.

Published under license by AIP Publishing. <https://doi.org/10.1063/5.0012384>

I. INTRODUCTION

As a promising next-generation photovoltaic materials candidate, hybrid halide perovskites possess a general formula of ABX_3 , wherein A presents methylammonium (MA), formamidinium (FA), or cesium (Cs); B is lead (Pb) or tin (Sn) cation; and X often presents halogen (I, Br, or Cl) anions.^{1–5} Within nearly one decade, hybrid halide perovskite-based photovoltaics have achieved incredible progress, which is originated from their superior optical and electronic properties, such as high light absorption coefficient ($\sim 10^5 \text{ cm}^{-1}$), balanced ambipolar carrier transport, long carrier diffusion lengths ($> 1 \mu\text{m}$), high charge mobility ($\sim 10 \text{ cm}^2 \text{ V}^{-1} \text{ s}^{-1}$), and low exciton binding energy ($\sim 10 \text{ meV}$) in polycrystalline perovskite absorbers.^{6–14} These excellent optical and electronic properties, combining with its superior defect tolerance, meet many of the requirements for a high-efficiency optoelectronic technology.^{15–18} Moreover, the tunable direct bandgap for perovskite absorbers from 1.2 to 3.0 eV obtained by simple composition engineering allows the fabrication of perovskite/silicon and all

perovskite tandem solar cells with theoretical photoelectric conversion efficiency (PCE) limit beyond 30%, surpassing the Shockley–Queisser efficiency limit of single-junction solar cells.^{19–23} Their nature abundance and solution processable fabrication compatibility enlightened the low-cost photovoltaic technology revolution, with competitive leveled cost of electricity (LCOE) than that of crystalline silicon solar cells.^{24–27}

However, by virtue of their soft nature,¹⁸ perovskite absorbers that processed from solution and annealed at relatively low temperatures often suffer from the rapid formation of defects during their preparation. Polycrystalline perovskite films are presented approximately five orders of magnitudes higher defects density than single crystal perovskite and conventional crystalline silicon.^{14,28} Even though superior defect tolerance in this materials system, numerous defects still restrict the development of perovskite photovoltaics into an advanced level. Therefore, deeper understanding and delicate manipulation of defects and its evolution are critical to enable higher efficiency and more stable perovskite semiconductor devices.^{29–32} Since the first report of perovskite solar cells in 2009,³

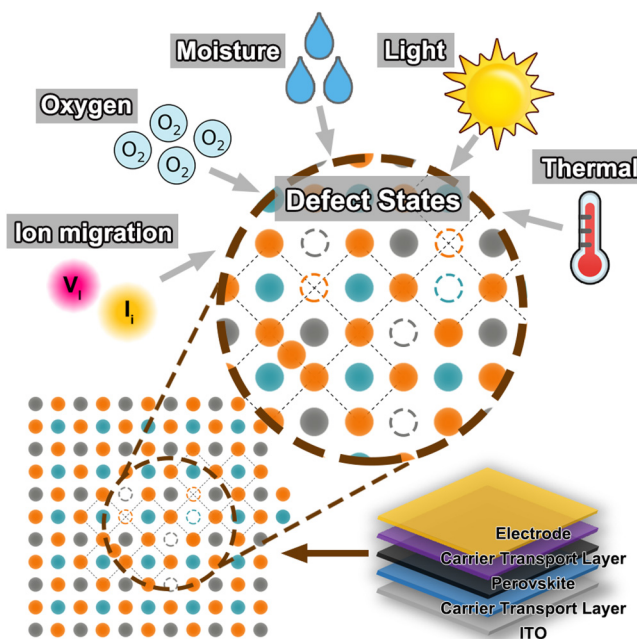
the studies with regard to high quality polycrystalline perovskite thin films with less defects have been broadly investigated based on various strategies: (1) the manipulation of primary precursors: component,^{30,33} stoichiometry,^{34,35} mixed solvent,^{36,37} and precursor purification;^{38,39} (2) the involvement of appropriate additives: Lewis acid and base,^{40,41} alkaline cations,^{30,33} chlorine,⁴² and water;⁴³ (3) the optimization of the fabrication process: solvent annealing,⁴⁴ Ostwald Ripening,³¹ and so on. Besides, many characterization methods to analyze defects density in perovskite films and corresponding devices have been developed, including space charge limited current (SCLC),^{29,45} thermal admittance spectroscopy (TAS),^{46,47} thermally stimulated current (TSC) measurement,^{17,48} deep-level transient spectroscopy (DLTS),³² absolute photoluminescence (PL) emission,⁴⁹ ideality factor (IF),⁵⁰ and recently proposed drive-level capacitance profiling (DLCP) approach.⁵¹ These efforts have largely underpinned the rapid development of perovskite solar cells, with the efficiency over 25%.

Nevertheless, the shortcomings in long-term stability of perovskite based photovoltaics became the dominant obstacle to further commercialization.^{52,53} Principally, hybrid halide perovskite absorbers are chemically unstable when exposed to moisture, light, or heat because of their low lattice energies and the existence of easily decomposed organic contents.^{52,54} Defects and defect related behavior, such as ion migration and the reaction with invasive molecule as a degradation trigger, are believed to play a vital role in the chemical degradation of perovskite materials. Recently, more complicated degradation pathways are observed, for example: (1) carrier transport materials induced degradation of perovskite absorbers^{55–58} and (2) reactions between the metal electrodes and halogens from perovskite films during prolonged operation.^{59,60} The interfaces between perovskite absorbers and charge transport layers enable more serious crisis of stability in perovskite photovoltaics under different aging stresses.^{61–64} Thus, several strategies have been presented to improve the long-term operational stability of perovskite solar cells, such as tuning the composition of the perovskite absorbers,^{30,65,66} optimizing the transport materials and interfaces,^{67–69} and employing more advanced encapsulation techniques.^{70–72}

Herein, we pay close attention to the origins of defect and its evolution in perovskite materials and underline the dominating interfacial defects problem between perovskite absorbers and carrier transport layers. We further discuss the recombination pathway at the interfaces and its effect on the efficiency deterioration. Moreover, we emphasize the influence of defects and defect related behavior in different degradation processes of perovskites, such as ion migration, the exposure to moisture, oxygen, light irradiation, and thermal stressors (Scheme 1). Particularly, recent significant strategies with regard to the defects manipulation facilitated both efficiency and stability improvement have been investigated deeply to provide a useful guidance for further breakthroughs of perovskite solar cells.

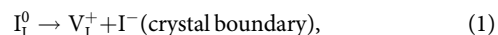
II. DEFECTS CHEMISTRY IN PEROVSKITE FILMS

The native point defects in crystalline semiconductor materials, such as silicon, gallium arsenide, and cadmium telluride, have been investigated extensively.^{73–75} Due to thermal fluctuations, some of the atoms can abandon their regular position in the lattice,



SCHEME 1. The illustration of interactions between defect states and ion migration, oxygen, moisture, light irradiation, and thermal stressors in hybrid halide perovskite solar cells.

leaving a defect site called vacancy. The imperfect atom could occupy the gap between the lattice points, which is called interstitial. Besides, a substitutional defect is formed as an atom from the original site is replaced with an impurity atom.⁷⁶ Two primary defect pairs, Schottky defects and Frenkel defects, were demonstrated to form in a crystal at thermal equilibrium.⁷⁷ Take a typical perovskite material MAPbI_3 as an example, the formation of the I Schottky defect was written as Eq. (1) and the formation of the I Frenkel defect pair was presented as Eq. (2),



where I_l^0 presents a I atom occupied its perfect site, V_l^+ presents a positively charged I vacancy defect, and I_i^- is a negatively charged I interstitial defect. Moreover, the point defect concentration in materials is related to the system thermodynamic temperature and their formation energy,⁷⁸ which depends on electronic chemical potential (related to the Fermi level, E_F) and atomic chemical potential (dominated by the reactants such as concentrations and activity). In other words, the stoichiometry and component of reactants, even the fabrication detail, could greatly influence the defects formation and concentration by altering the reaction chemical potentials. Thus, it is fundamental and critical to control the crystal growth conditions to suppress the detrimental defect states in perovskite semiconductors.

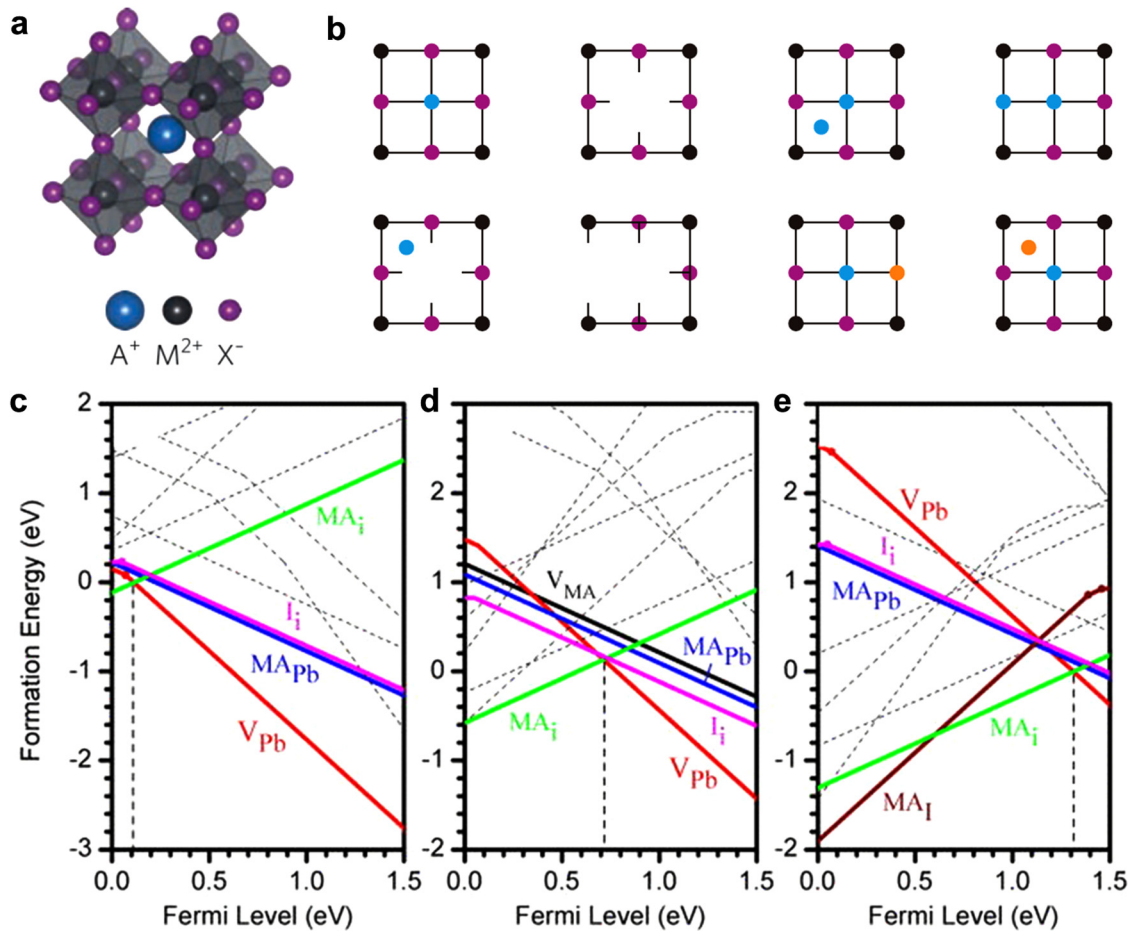


FIG. 1. (a) Schematic representation of the MAPbI_3 unit cell. (b) Illustration of perfect lattice, vacancy, interstitial, anti-site substitution, Frenkel defects pair, Schottky defects pair, substitutional, and interstitial impurity.¹⁸ Reproduced with permission from Ball and Petrozza, Nat. Energy 1, 16149 (2016). Copyright 2016 Nature Publishing Group. (c)–(e) The calculated formation energies of intrinsic point defects in MAPbI_3 at different chemical potentials.¹⁶ Reproduced with permission from Yin *et al.*, Appl. Phys. Lett. **104**, 063903 (2014). Copyright 2014 AIP Publishing LLC.

Recently, numerous theoretical calculations have investigated the defect states in the most common used MAPbI_3 perovskite [Fig. 1(a)]. To be noted, the native point defects in MAPbI_3 include the vacancies V_{MA} , V_{Pb} , and V_{I} ; the interstitials MA_{i} , Pb_{i} , and I_{i} ; antisite substitutions Pb_{MA} , I_{Pb} , I_{MA} , and MA_{I} ; and cation substitutions Pb_{MA} , and MA_{Pb} [Fig. 1(b)].¹⁸ It is generally believed that in perovskites, defects with low formation energies, implying their easy formation, have shallow energy levels near the valance band maximum or the conduction band minimum, while some defects that contributed to deep energy levels in the bandgap have high formation energies [Figs. 1(c)–1(e)].^{15,16,61,79} The superior defect tolerance originates from the antibonding nature of the electronic band edges and effective dielectric screening in the perovskite materials. These properties ensure the promise of perovskite as light absorber in photovoltaics with great progress in efficiency.^{17,18}

In addition to traditional MAPbI_3 , FAPbI_3 , CsPbI_3 , and their hybrid halide compositions are also the most attractive perovskite absorbers and have achieved the significantly improved efficiency recently.^{54,56} The density functional theory (DFT) calculation has confirmed the similar energy levels of these defects in FAPbI_3 , when comparing with that in MAPbI_3 , except that antisites (FA_{I} and I_{FA}) create deep levels within bandgap in FAPbI_3 due to their much lower formation energies.⁸⁰ Li *et al.* found that V_{Pb} and V_{I} have the lowest formation energy among all acceptor and donor defects, respectively, under Pb-rich conditions in α -phase CsPbI_3 .⁸¹ Huang *et al.* confirmed that most of the intrinsic defects induce deeper transition energy levels in δ -phase CsPbI_3 , compared with that in γ -phase CsPbI_3 .⁸² Recently, Dunfield *et al.* connected the defect tolerance with the structural stability, namely, the tolerance factor of perovskite materials.⁸³ MAPbI_3 , CsPbBr_3 ,⁸⁴ CsSnI_3 ,⁸⁵ and MAPbBr_3 ⁸⁶ have structural tolerance factors of roughly 0.82–0.85,

whereas FAPbI_3 , CsPbI_3 , FASnI_3 , and MASnI_3 ⁸⁷ outside this range. Interestingly, the formers have defect tolerance in their lowest energy phase, whereas the latter have not. Meanwhile, this connection gives a reasonable explanation for the obvious increase of formation energy for deep-level defects (F_{AI} and I_{FA}) in FAPbI_3 by alloying roughly half of the FA cations with MA to form $\text{FA}_{0.52}\text{MA}_{0.48}\text{PbI}_3$.⁸⁰ This alloying strategy reduces the tolerance factor of perovskite absorbers to roughly 0.84, which improve the structural stability and thus enable perovskite to become more defect tolerant.

Beyond the point defects in the bulk, the defects located in grain boundary and surface in polycrystalline perovskite films often present more complicated structural and chemical environment, which largely determined the recombination dynamics and materials stability of perovskite solar cells.^{6,17,88–91} It is easy to understand that various defects, such as V_{MA} , V_{I} , uncoordinated Pb^{2+} or I^- ions, Pb or I clusters, Pb–I antisite defects, are likely to

exist in the grain boundary and film surface. Specifically, apart from the common defects with the shallow energy level, such as MA and I vacancies, Agiorgousis *et al.* revealed that the strong covalency of Pb^{2+} ions could induce the formation of Pb clusters, which has deep energy levels within the bandgap and low formation energy [Figs. 2(a) and 2(b)].⁹⁰ Also, Pb_i antisite defect is proved to hold a deep transition level within the bandgap, while its formation energy is low enough to contribute a high density of recombination centers under iodine-rich conditions [Figs. 2(c) and 2(d)].⁹¹ In addition, the excess iodine in the form of I_i is proved as detrimental deep defects in MAPbI_3 . It is efficient at trapping holes, which is associated with the formation of favorable I–I interactions. The appropriate control of oxidizing conditions during and after the perovskite fabrications could covert these harmful defects to long-lived, kinetically inactive electron defects [Fig. 2(e)].^{86,92} Such defects at the surfaces and grain boundaries

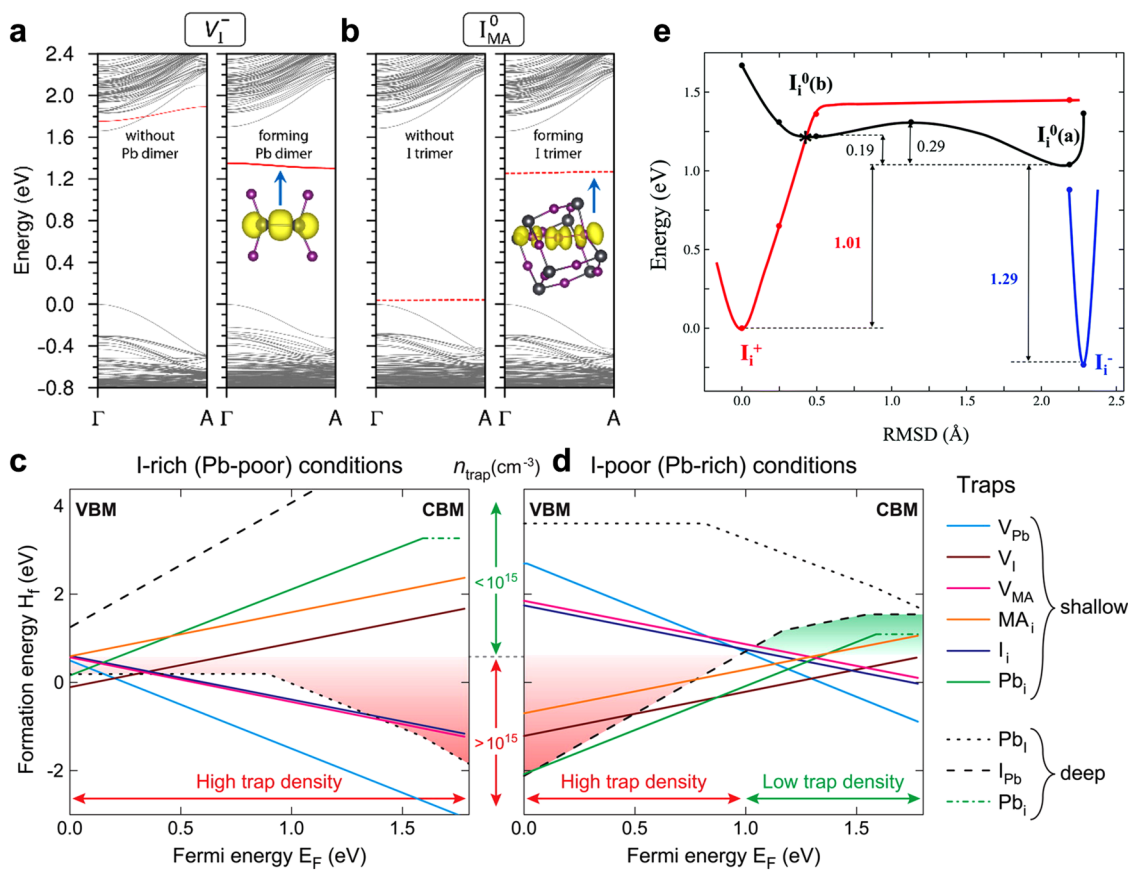


FIG. 2. (a) and (b) Band structure plot for V_I^- and I_{MA}^0 from Γ to $(1/2, 1/2, 1/2)$. After forming Pb dimer and I trimer, the defect occupied band in the bandgap is shown by a thick red line. The insets show the charge density contour plot for the defect bands after forming Pb dimers and I trimers.⁹⁰ Reproduced with permission from Agiorgousis *et al.*, J. Am. Chem. Soc. **136**, 14570 (2014). Copyright 2014 American Chemical Society (ACS) Publications. (c) and (d) The formation energies and volume densities of key defects in perovskites. Defect formation energies for iodine-poor and iodine-rich growth conditions.⁹¹ Reproduced with permission from Buin *et al.*, Nano Lett. **14**, 6281 (2014). Copyright 2014 ACS Publications. (e) Configuration diagrams (energy vs structural coordinates) of interstitial iodine in its positive (red), neutral (black), and negative (blue) charge states vs the root mean square displacement (RMSD).⁸⁶ Reproduced with permission from Meggiolaro *et al.*, Energy Environ. Sci. **11**, 702 (2018). Copyright 2018 The Royal Society of Chemistry.

of perovskite film serve as severe non-radiative recombination centers, which are detrimental to its photovoltaic performance. Recently, nanoscale defect clusters have been experimentally observed at grain boundaries and compositionally distinct entities in perovskite absorbers. The authors also reveal a hole-trapping character with the kinetics limited by diffusion of holes to the local defect clusters, suggesting the performance-limiting of defect clusters at grain boundary and interfaces.⁹³

III. INTERFACE DEFECTS AND DEFECTS RECOMBINATION IN PEROVSKITE SOLAR CELLS

For photovoltaic devices, the detailed balance of carrier generation and recombination during operation determines its performance.^{94–97} The main carrier recombination pathways in perovskite solar cells include radiative recombination, defect-assisted recombination, and Auger recombination, while the latter two contribute to the non-radiative recombination loss [Fig. 3(a)].⁹⁷ Besides, Auger recombination predominantly occurs at high carrier injection concentrations ($>10^{17} \text{ cm}^{-3}$). It was recently reported that much weaker Auger recombination exists and has a negligible influence on perovskite solar cells, in contrast to that in crystalline silicon solar cells [Figs. 3(b) and 3(c)].⁹⁸ Whereas the defect-assisted Shockley–Read–Hall (SRH) recombination, depending on the energy level depth and density of defect states, dominated the

primary non-radiative recombination loss in perovskite solar cells.^{18,74} In general, when an active defect state energetically lies within the bandgap, it probably captured or trapped an approaching electron or hole. If the energy level of this defect is shallow enough (within $\sim kT$ from band edges, and k is the Boltzmann constant), the trapped carrier is likely to detrap or emit with the help of phonon absorption. However, in the case of the deep-level defects, the trapped carrier would need to annihilate until recombine with an opposite charge and emitted,⁹⁵ which is, in particular, of fundamental importance to photovoltaic performance under open-circuit conditions.

As a typical thin film photovoltaic device, the perovskite solar cell is usually structured by a perovskite layer, electron transport layer, hole transport layer, and electrodes [Fig. 3(d)].⁹⁹ Reasonably, many defect states in the interfaces between perovskite film and transport layers incredibly complicate the carrier recombination events since the severe defects issue have been demonstrated at the grain boundary and surface of perovskite films as discussed above.^{88,100} Furthermore, Sarritzu *et al.* have investigated the microscopic origin of non-radiative recombination events in perovskite based heterojunctions through all-optical technique. They highlighted defect-assisted SRH recombination as the main decay process and quantified the additional efficiency degradation due to minority carriers recombination [Fig. 3(e)].⁵⁰ The minority carrier recombination is another severe recombination pathway as perovskites connected with the carrier transport

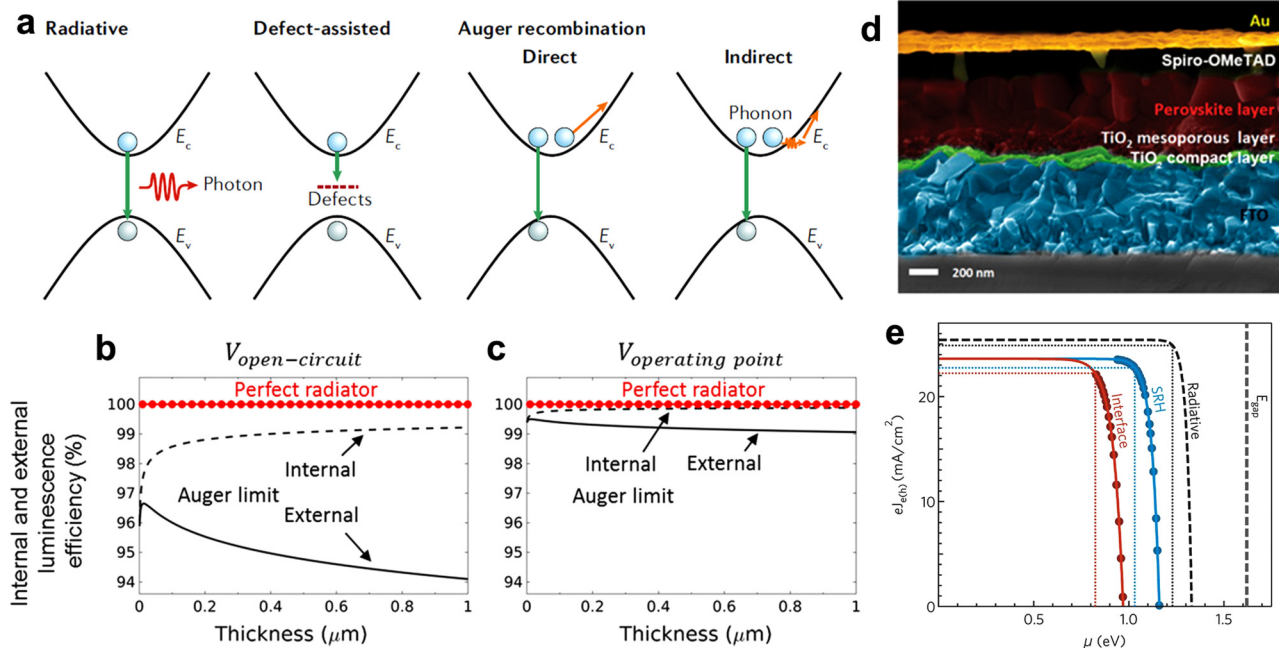


FIG. 3. (a) Generalized recombination pathway of photogenerated carriers, including radiative, defect-assisted, Auger and indirect recombination.⁹⁷ Reproduced with permission from Luo *et al.*, Nat. Rev. Mater. **5**, 44 (2019). Copyright 2019 Nature Publishing Group. (b) and (c) External and internal luminescence efficiencies in the Auger limit, both in open-circuit and at the operating point under illumination.⁹⁸ Pazos-Onut *et al.*, J. Phys. Chem. Lett. **9**, 1703 (2018). Copyright 2018 Author(s), licensed under an ACS AuthorChoice License. (d) The cross-sectional scanning electron microscope image of the perovskite solar cells.⁹⁹ Bi *et al.*, Sci. Adv. **2**, 1501170 (2016). Copyright 2016 Author(s), licensed under a Creative Commons Attribution (CC BY) license. (e) The influence of radiative, SRH, and interface recombination on photovoltaic parameters.⁵⁰ Sarritzu *et al.*, Sci. Rep. **7**, 44629 (2017). Copyright 2017 Author(s), licensed under a Creative Commons Attribution (CC BY) license.

layers, which originates from the imperfect or unmatched band alignment.^{84,96} Therefore, it is necessary to reduce the recombination loss at interfaces between perovskite absorbers and carrier transport layers to boost the photovoltaic performance of the final device close to the radiative limit.¹⁰⁰

Recently, several important strategies with regard to interface modification to suppress the recombination loss at interface have been reported. Jiang *et al.* introduce an organic halide salt phenethylammonium iodide (PEAI) at the interface between FAMA mixed perovskite absorber and hole transport layer for defect passivation. They infer that I⁻ vacancies at the grain boundary and surface of perovskite films could be effectively passivated, which contribute to suppressed non-radiative recombination and improved performance [Figs. 4(a)–4(d)]. To be noted, a certified efficiency of 23.32% and open circuit voltage (V_{OC}) of 1.18 V are obtained.¹⁰¹ Moreover, in view of most passivator currently used to mitigate defects, they often form poorly conductive aggregates at the perovskite interface with the carrier transport layer, impeding the extraction of photogenerated charge carriers. Thus, 4-*tert*-butyl-benzylammonium iodide (tBBAI) is employed to effectively suppress defects on the surface of perovskite films, because the bulky *tert*-butyl groups prevent the detrimental aggregation by steric repulsion [Figs. 4(e)–4(h)]. Beyond PEAI, tBBAI could significantly accelerate the charge extraction from the perovskite layer into hole transporter and its modification boosts the efficiency from ~20% to 23.5%.¹⁰² In addition, Yoo *et al.* declare that the isopropanol, as a protic polar solvent, could destabilize the perovskite absorber and cause an undesirable degradation of device properties. They thus employ a unique precursor/solvent combination (linear

alkyl ammonium bromides/chloroform) to passivate interfaces and grain boundary defects effectively, which improve the performance of perovskite solar cells to 23.4% (certified and stabilized 22.6%) [Figs. 5(a)–5(c)]. The highest electroluminescence external quantum efficiency up to 8.9% is achieved in optimized solar cells.¹⁰³ On the other hand, absolute photoluminescence (PL) intensity and derived quasi-Fermi level splitting (QFLS) are involved in the visualization of interface recombination and its cure.^{49,97,100} Stolterfoht *et al.* found that inserting two kinds of ultrathin interlayers (PFN-P2 and LiF) allows a substantial reduction of interface-induced recombination losses at both interfaces between the perovskite and transport layers, which increases the V_{OC} of the optimized p-i-n-type solar cells to 1.17 V [Figs. 5(d)–5(g)].⁴⁹

Although great advance has achieved to mitigate interface recombination loss, little is known about how these interlayers work on the microscopic or atomic level. For instance, the suppression of defect-assisted SRH recombination and minority carrier recombination at interfaces is difficult to distinguish well.^{96,97,100} The specific defects passivation mechanism at grain boundary and surface is not clear enough. In this scenario, Zheng *et al.* consider the ionic nature of perovskite materials and defects are usually negatively charged or positively charged.^{62,104} They proposed several kinds of quaternary ammonium halide salts (such as l- α -phosphatidylcholine, choline iodide, and choline chloride) to simultaneously passivate the negatively and positively charged defects in perovskite films [Figs. 5(h)–5(j)]. But to be noted, the types and behavior of defects at interface still complicated, which is sensitive to the film formation process, even carrier transport materials. Whether the passivation only follows the

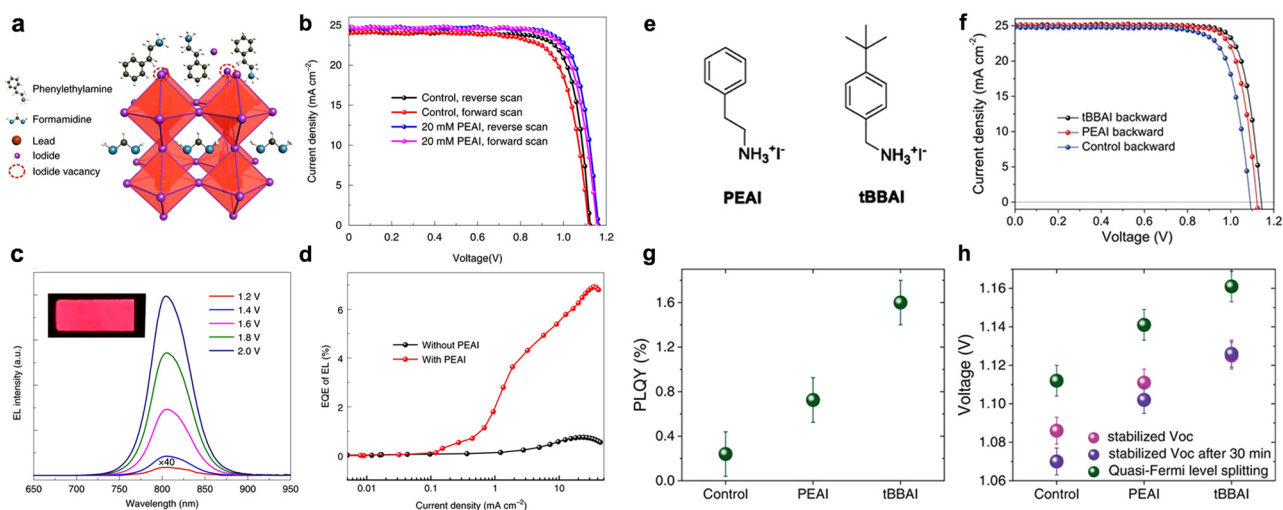


FIG. 4. (a) Possible passivation mechanism of the PEAI layer for the perovskite film. (b) The typical J-V curve of the device with PEAI (20 mM) and without PEAI treatment. (c) EL spectra of the devices with PEAI under different voltage bias operating as LEDs. Inset: EL image of the devices under different voltage bias. (d) The external quantum efficiency (EQE) of EL of the devices while operating as LEDs.¹⁰¹ Reproduced with permission from Jiang *et al.*, Nat. Photonics **13**, 460 (2019). Copyright 2019 Nature Publishing Group. (e) Chemical structures of PEAI and tBBAI. (f) Reverse J-V curves of champion devices. (g) PLQY and (h) stabilized V_{OC} and quasi-Fermi level splitting for the layer structure glass/FTO/c-TiO₂/mp-TiO₂/perovskite/interface layer/HTL. The stabilized V_{OC} after 30 min light soaking is also shown.¹⁰² Reproduced with permission from Zhu *et al.*, Adv. Mater. **32**, 1907757 (2020). Copyright 2020 Wiley-VCH.

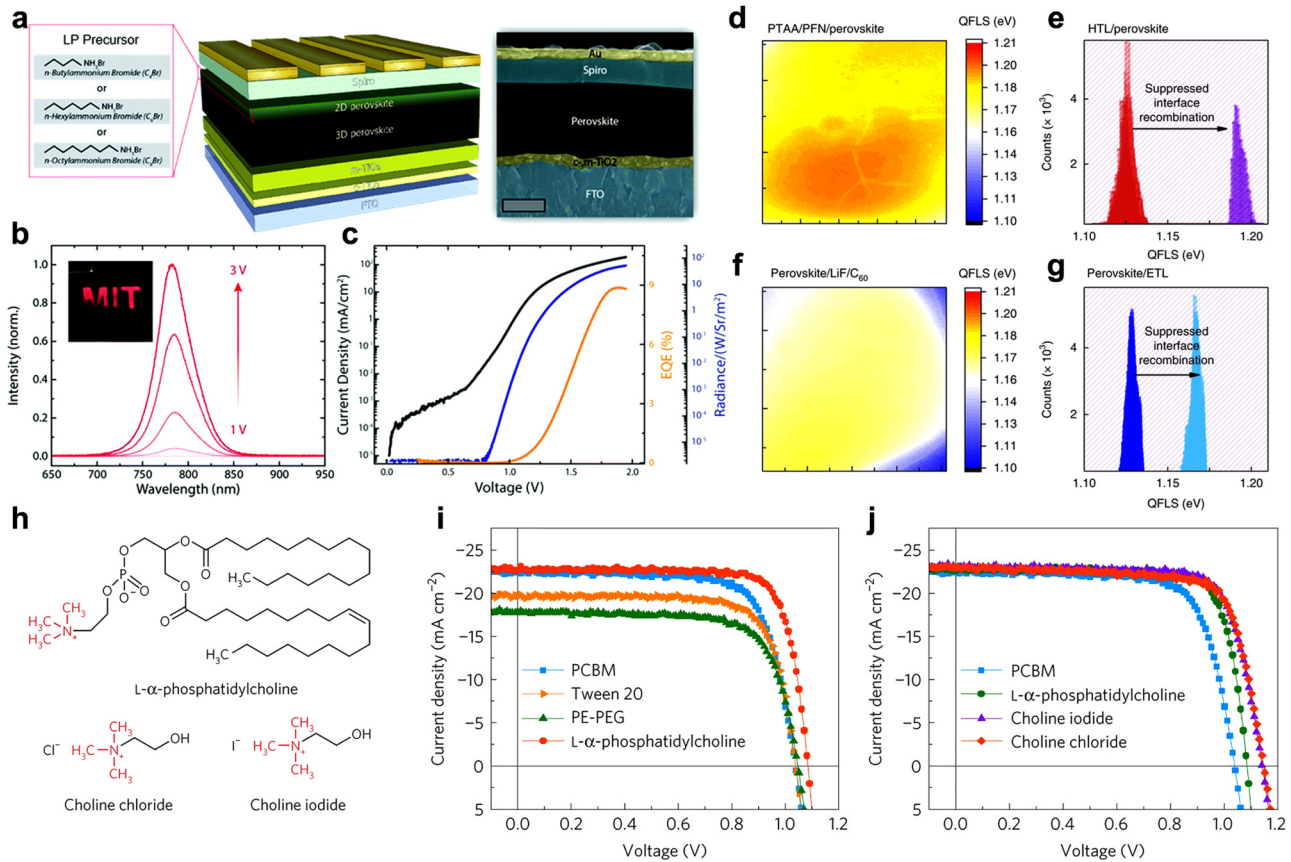


FIG. 5. (a) Schematic illustration of optimized perovskite solar cells with false colored cross-sectional SEM (scale bar: 500 nm). (b) Electroluminescence spectra of optimized devices operated as a LED. (c) Plot of current density, EQE, and radiance as a function of voltage. The device shows a max EQE of 8.9%.¹⁰³ Yoo et al., Energy Environ. Sci. **12**, 2192 (2019). Copyright 2019 Author(s), licensed under a Creative Commons Attribution (CC BY) license. The QFLS maps (d, f) and histograms (e, g) of a PTAA/PFN-P2/perovskite and perovskite/LiF/C₆₀ film on glass, implying a comparatively high average QFLS of 1.19 and 1.169 eV.⁴⁹ Reproduced with permission from Stolterfoht et al., Nat. Energy **3**, 847 (2018). Copyright 2018 Nature Publishing Group. (h) Chemical structures of L-phosphatidylcholine, choline iodide, and choline chloride. (i) and (j) The $J-V$ curves of two-step-processed MAPbI₃ devices with different passivation layers: PCBM, Tween 20, L-phosphatidylcholine, PE-PEG, choline chloride, and choline iodide.¹⁰⁴ Reproduced with permission from Zheng et al., Nat. Energy **2**, 17102 (2017). Copyright 2017 Nature Publishing Group.

coulomb mechanism still needs further exploration.¹⁰⁴ Therefore, it is urgent to develop appropriate characterization or theoretical calculation in the context of the defects passivation at grain boundary and surface of perovskite films.

IV. DEFECTS DOMINATED INSTABILITY IN PEROVSKITE SOLAR CELLS

Despite the progress achieved in efficiencies of perovskite solar cells, severe stability issue hindered its large-scale fabrication and commercialization.^{52–54,59,83} It has been generally observed several drawbacks responsible for the degradation of perovskite solar cells, including internal factors (e.g., structure, composition, and defects) and the interaction with external environment (e.g., moisture,^{105–108} oxygen,^{64,109} temperature,^{52,55} and illumination^{57,110}). In particular, the degradation process of perovskite

solar cells became more intricate under the influence of multiple factors simultaneously.^{57,106} For example, the device with encapsulation under real work condition (maximum power point, MPP) suffers from all factors mentioned above. The prolonged illumination leads to the accumulation of heat, followed by the rise up of operation temperature. Besides, the ideal encapsulation technology can isolate most of oxygen and moisture from perovskite films effectively; however, it is inevitable to leave a tiny amount of oxygen and moisture in perovskite films, which may come from any step in the preparation process.⁹⁴ Also, ion migration^{111–113} is unavoidable under MPP operation, which needs to be addressed carefully. Although the solution to overcome the instability issue of perovskite solar cells is complicated that involves many comprehensive factors, a deeper understanding with regard to degradation mechanism originated from defects and their evolution under different aging stresses will be great helpful.

A. Ion migration and defects

Ion migration¹³ have attracted considerable interest from the community, as it becomes the possible origin of many unusual phenomenon in perovskite materials and corresponding photovoltaic devices, such as current density–voltage (J – V) hysteresis,^{47,114–117} band bending,¹¹⁸ giant dielectric constant,¹¹⁹ photoinduced phase separation,^{120,121} and self-poling effect.¹⁷ Recently, it has been reported that ion migration accelerates the degradation process by facilitating the decomposition reaction at interfaces,^{62,122,123} and it attracted increasing attention to further investigate the underlying mechanism. Eames *et al.* found that defects, particularly vacancies and interstitials, introduce the ion migration channels in perovskite films [Figs. 6(a)–6(c)], acting as shuttles for halides hopping. In addition, a strict connection is highlighted between the energies of defects formation and the entity of ion migration.¹²⁴ Many theoretical calculations contribute to the activation energies (E_A) for ion/defect migration in perovskite films.^{63,89,125–127} The calculated values present a significant variation, ranging from ~ 0.1 to ~ 0.6 eV for iodine defects, similar to the large variation in the measured values ranging from ~ 0.1 to ~ 1.0 eV from experiment.^{111,128,129} However, these results reveal the same order of activation energies consistently, in which halide defects are moving faster than A

cations, and A cations are in turn faster than lead defects. Moreover, it has been reported that interstitial hydrogen could migrate in MAPbI_3 along a transient hydrogen bond connecting two equatorial iodides with a low barrier of 0.29 eV [Fig. 6(d)].¹³⁰ Experimentally, the extrinsic ions (e.g., Li^+ , Na^+) were found to migrate in perovskite films [Figs. 6(e) and 6(f)].¹¹² Recently, Meggiolaro *et al.* investigated the influence of grain size in perovskite films on the ion migrations and activation energies. The result indicates that the ion migration is dominant at surface and grain boundaries in perovskite films due to the surface assisted formation of migrating defects.⁸⁹ Moreover, Phung *et al.* present that the grain boundaries inhibited the lateral migration of defects, evidenced by the time evolution of spatially resolved photoluminescence profiles, underlining the interaction between light induced migrated defects with grain boundaries.¹³¹ Particularly, Weber *et al.* have demonstrated the fast formation and slow release dynamics of the localized interfacial charge in perovskite solar cells due to defects migration and accumulation at interfaces after switching on/off the applied voltage by employing time-resolved Kelvin probe microscopy experiments. This asymmetry in the dynamics is responsible for the current–voltage hysteresis of perovskite solar cells, instead of the slow migration of mobile defects.¹³² Consistently, Caddeo *et al.*

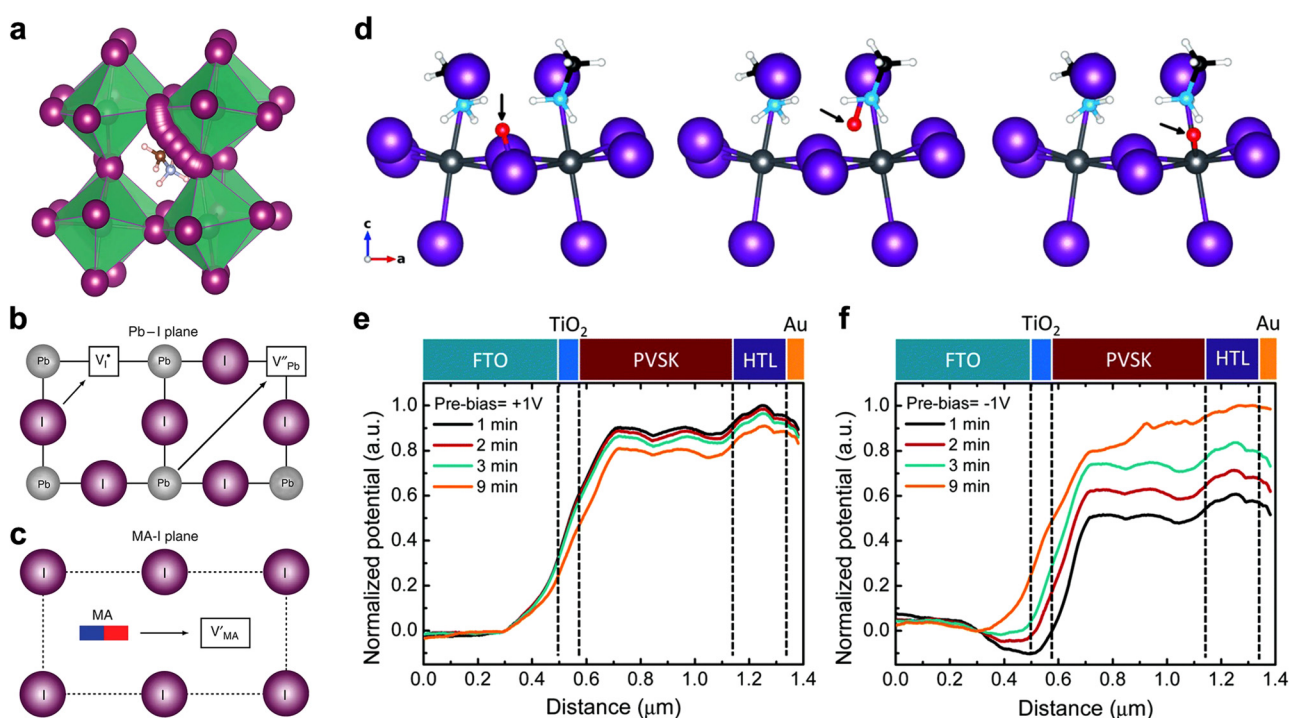


FIG. 6. (a) Calculated migration path indicating a slightly curved path. (b) and (c) Schematic illustration of the three ionic transport mechanisms involving conventional vacancy hopping between neighboring positions.¹²⁴ Eames *et al.*, Nat. Commun. **6**, 7497 (2015). Copyright 2015 Author(s), licensed under a Creative Commons Attribution (CC BY) license. (d) Fully optimized positions of H^+ (left), H^0 (center), and H^- (right) in otherwise unrelaxed MAPbI_3 lattice, the interstitial hydrogen defect is enlarged, red, and marked by an arrow.¹³⁰ Egger *et al.*, Angew. Chem. Int. Ed. Engl. **54**, 12437 (2015). Copyright 2015 Author(s), licensed under a Creative Commons Attribution (CC BY) license. (e) and (f) Cross-sectional Kelvin probe force microscopy potentials of perovskite solar cells after positive and negative poling.¹¹² Reproduced with permission from Li *et al.*, Energy Environ. Sci. **10**, 1234 (2017). Copyright 2017 The Royal Society of Chemistry.

demonstrated the similar result by molecular dynamics simulations.¹³³ These results implied two possible solutions to the hysteresis, including the suppression of ion migration and the facilitation of release dynamics for localized interfacial charge at interfaces, which further highlight the vital position of surfaces and grain boundaries in efficiency and stability of perovskite solar cells.

B. Moisture and defects

Water as an effective assistant to improve the crystal quality of perovskite films during the fabrication process have been widely accepted;^{43,134} however, the moisture induced decomposition of perovskite through specific chemical interactions is also irrefutable. Leguy *et al.* have demonstrated the reversible formation of hydrated MAPbI₃ phases when exposed to water vapor due to the hygroscopic MA [Figs. 7(a) and 7(b)].¹⁰⁷ Moreover, it is sensitive to lead to irreversible degradation of hydrated MAPbI₃ triggered by the light or a tiny excess water. Ahn *et al.* found trapped charges induced by defects at grain boundaries and surfaces of perovskite films under illumination provide charge accumulation sites and infiltration pathways, which are responsible for triggering the irreversible degradation

under moisture exposure regardless of charge polarity. Also, the trapped charges from corona discharge or electrical injection could accelerate this irreversible degradation [Figs. 7(c)–7(e)].¹³⁵ The synergistic effect of oxygen and water on moisture-induced degradation was also found. Wang *et al.* observed that the defective grain boundaries with a high density of trapped charges facilitate the quick permeation of moisture. The degradation rates in the moisture environment are sensitive to the grain sizes, evident by five kinds of perovskite films with different deposition methods [Figs. 7(f)–7(h)].¹⁰⁵ Thus, beyond their influence on photovoltaic performance, defects at grain boundaries and surfaces play a decisive role in moisture induced degradation of perovskite films and corresponding devices.

C. Oxygen and defects

Similar to the case of moisture, oxygen is also one of the major degradation triggers of perovskite solar cells. Early studies have indicated that the degradation of perovskite films is not severe when it exposed only to oxygen. However, other factors, like illumination, applied current or electrical bias greatly accelerate the

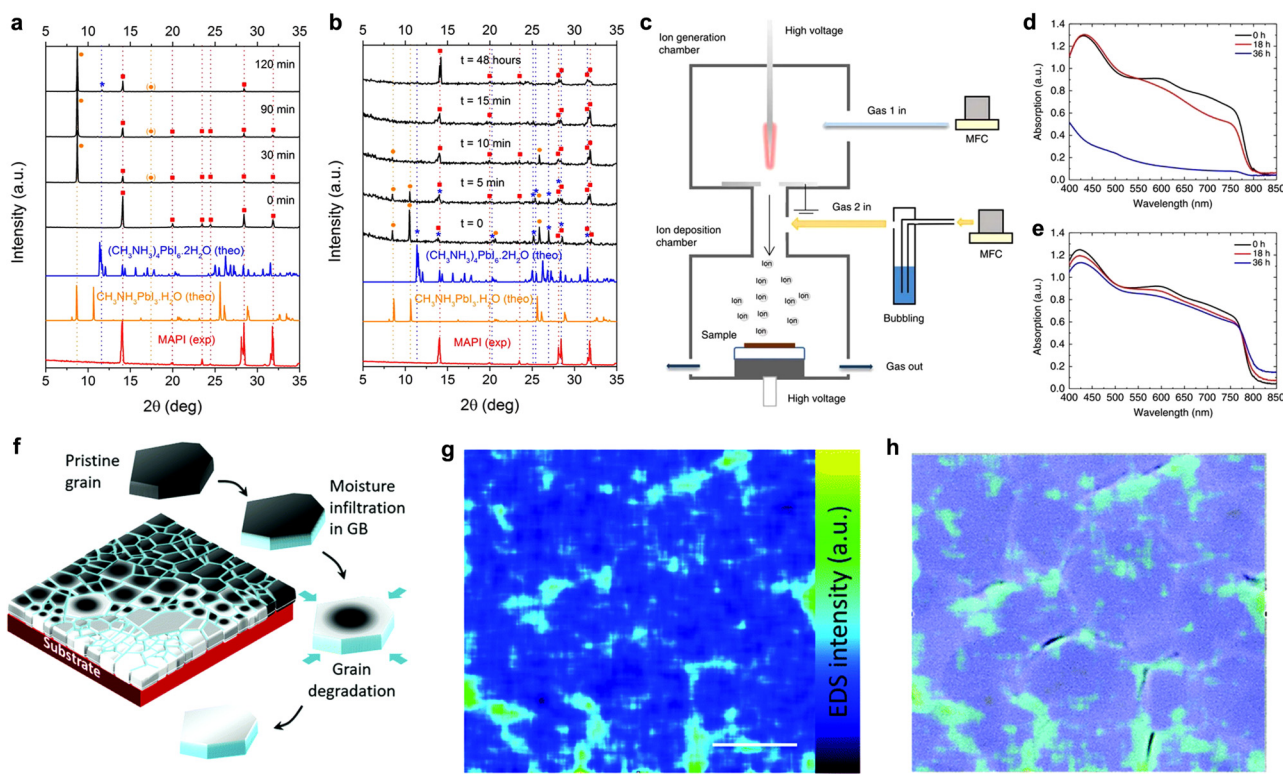


FIG. 7. Time-resolved XRD patterns of polycrystalline MAPbI₃ films: (a) hydration of a MAPbI₃ film and (b) dehydration of directly synthesized hydrated crystals.¹⁰⁷ Reproduced with permission from Leguy *et al.*, Chem. Mater. **27**, 3397 (2015). Copyright 2015 ACS Publications. (c) Experimental setup of corona discharge for ion generation. Absorption spectra of the perovskite films measured during deposition of (d) positive nitrogen ions and (e) negative hydrogen ions at 40% RH.¹³⁵ Ahn *et al.*, Nat. Commun. **7**, 13422 (2016). Copyright 2016 Author(s), licensed under a Creative Commons Attribution (CC BY) license. (f) Schematic diagram showing the degradation of the perovskite film in moisture. (g) The distributions of elemental oxygen in the film. (h) Overlay of EDS mapping image with the corresponding STEM image.¹⁰⁵ Reproduced with permission from Wang *et al.*, Energy Environ. Sci. **10**, 516 (2017). Copyright 2017 The Royal Society of Chemistry.

oxygen-induced decomposition of perovskites.⁵⁷ Aristidou *et al.* demonstrate the exposure of MAPbI₃ films to oxygen under illumination leads to the formation of reactive superoxide (O₂⁻) through electron transfer from photoexcited perovskite to molecular oxygen.¹³⁶ Then, this degradation is initiated by the deprotonation reaction of O₂⁻ with the MA⁺ of the perovskite absorber, leading to the degradation products with PbI₂, MA, I₂, and water [Fig. 8(a)]. Further theoretical calculation reveals that the negatively charged V_I defects binding with oxygen have the lowest formation energy, implying its preferred sites in mediating the photoinduced formation of O₂⁻ from oxygen [Fig. 8(b)]. The V_I defects involved reaction promotes the fast diffusion of oxygen from surface into the interior of perovskite films.⁶⁴ Moreover, this degradation is reported to be slowed down when the devices operated under short-circuit conditions, rather than open-circuit. This is because of the competition process of the extraction of photo-generated electrons and reactions of negatively charged V_I defects with oxygen to form O₂⁻.¹⁰⁹ In addition, the oxygen induced degradation reveals a similar grain boundary effect with that of moisture. Straightforward, it is demonstrated that the perovskite films with larger grain size, indicative of less grain boundaries and defects density, exhibited lower rates of the formation of O₂⁻ and degradation, when compared with that of smaller grains.⁶⁴ Therefore, it highlights that defects at surfaces and grain boundaries also play a key role in oxygen induced degradation of perovskite films and corresponding devices.

D. Light irradiation and defects

The instability of perovskite solar cells under light irradiation, particularly ultraviolet (UV) light, have been considered early, because of the photocatalytic effect from widely used electron transport materials TiO₂.^{137,138} It is demonstrated that the photocatalytic effect generates defects at the interface, which is one of the main reasons for the device degradation [Fig. 8(c)].¹³⁹ Moreover, light irradiation serves as an accelerator in the degradation process of perovskite solar cells. First, light irradiation can greatly decrease the energy barrier for ion migration and expedite vacancy-mediated ion migration in perovskite films,¹⁴⁰ which is related with the excess charge carriers and defects with carrier trapped under illumination.¹⁴¹ However, ion migration is difficult to detect within the perovskite single crystal, because it is much lower defect density determines a much higher energy barrier for ion migration, even under illumination.¹⁴² Besides, phase segregation and thus the formation of I-rich and Br-rich domains in perovskite films are also accelerated under illumination^{143,144} due to its nature of vacancy-mediated halide ion migration [Fig. 8(d)].¹²¹ Severe degradation of perovskite solar cells, which originated from the ion migration and phase segregation under long-term illumination, has been experimentally confirmed.¹⁴⁵ Furthermore, it is worth mentioning that the light-moisture induced irreversible decomposition and light-oxygen dominated degradation process have been discussed above. Hence, reducing the trapped charge by

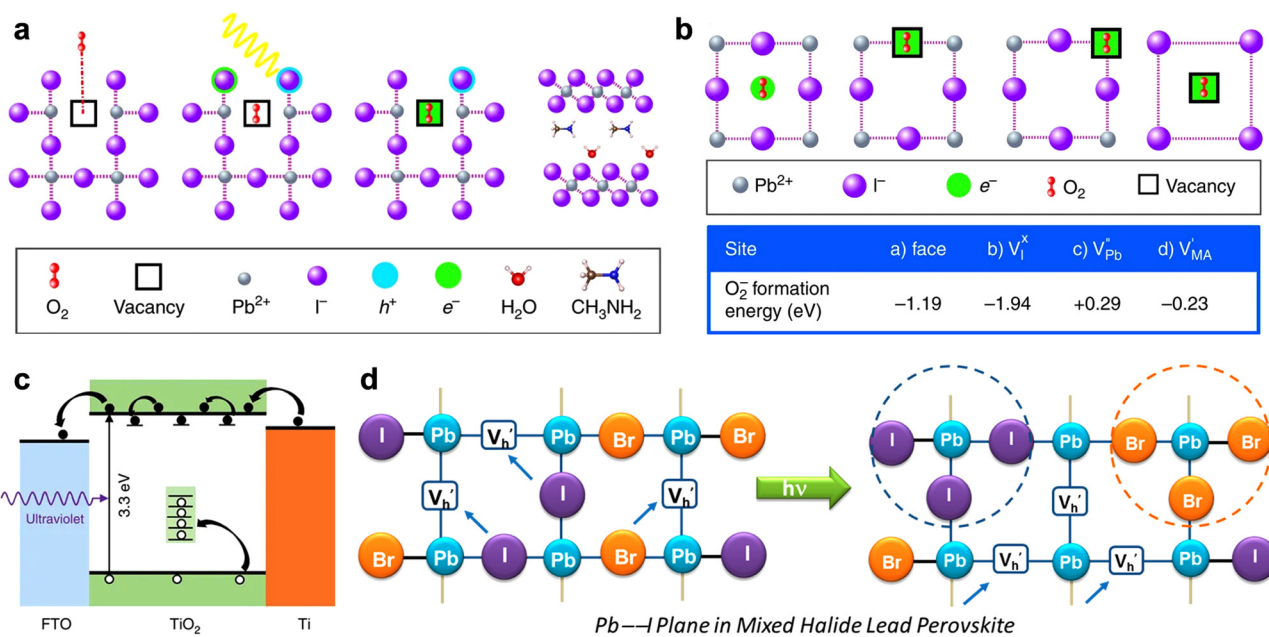


FIG. 8. (a) Schematic representation of the reaction mechanism of O₂ with MAPbI₃. (b) Schematic representation of possible O₂ binding and reduction sites in MAPbI₃ ([001] plane) and superoxide formation energy.⁶⁴ Aristidou *et al.*, Nat. Commun. **8**, 15218 (2017). Copyright 2017 Author(s), licensed under a Creative Commons Attribution (CC BY) license. (c) A schematic of the mechanism of defect-mediated photoconductivity in the TiO₂ thin film.¹³⁹ Li *et al.*, Nat. Commun. **7**, 12446 (2016). Copyright 2016 Author(s), licensed under a Creative Commons Attribution (CC BY) license. (d) Schematic representation of halide vacancies in the Pb—I plane of perovskite films, which influences halide ion migration and ultimately leads to I-rich and Br-rich domains.¹²¹ Yoon *et al.*, ACS Energy Lett. **2**, 1507 (2017). Copyright 2017 Author(s), licensed under an ACS AuthorChoice License.

passivation of defects in perovskites and interfaces is crucial in improving its light irradiation stability.

E. Thermal effect and defects

Temperature dependent crystal structure and phase behavior have a major impact on the thermal stability of perovskite absorbers, which is largely related to the structural characteristics and its Goldschmidt tolerance factor.¹⁴⁶ It has been reported that MAPbI₃ compounds are more structurally stable than their FAPbI₃ and CsPbI₃ counterparts [Fig. 9(a)] at room temperature.¹⁴⁷ However, MAPbI₃ are less resistant to thermal stressor compared to the latter ones because of its increased volatility and larger tendency to release a proton. It thus motivates the attempt to stabilize alternative compounds through A-site, B-site, or X-site hybridizing strategies [Fig. 9(b)].⁵⁸ Moreover, the thermal decomposition of perovskite films starts from its grain boundaries and surfaces, and the decomposition temperature is strongly related with defects density.^{17,47} It has been reported that MAPbI₃ single crystal with a low defect density of 10⁹–10¹¹ cm⁻³ decomposes at 240 °C; however, polycrystalline films with a high defect density of 10¹⁵–10¹⁷ cm⁻³ are verified

to start decomposition at normally 150 °C.^{148–150} This highlights the important role of defect states in thermal decomposition of perovskite films, and reducing the defect density contributes to the enhancement of thermal stability in perovskite solar cells. In addition, ion/defect migration is also highly dependent on temperature in perovskites. It was reported that migration of I related defects (both V_I and I_I) is improved at elevated temperature [Fig. 9(c)].¹²⁷ To be noted, high temperature facilitates the diffusion of extrinsic ion in carrier transport layer and metal counter electrode, which bring about the ohmic contact and device architecture degradation, greatly shaking the foundations of stability in perovskite solar cells.

V. STRATEGIES TO IMPROVE STABILITY IN PEROVSKITE SOLAR CELLS

In addition to identifying the main causes of degradation processes of perovskite solar cells, it is more crucial to improve the stability by effective strategies to an extent that will make the technology attractive from a commercial standpoint. In this section, we review many recently reported effective strategies, with regard to

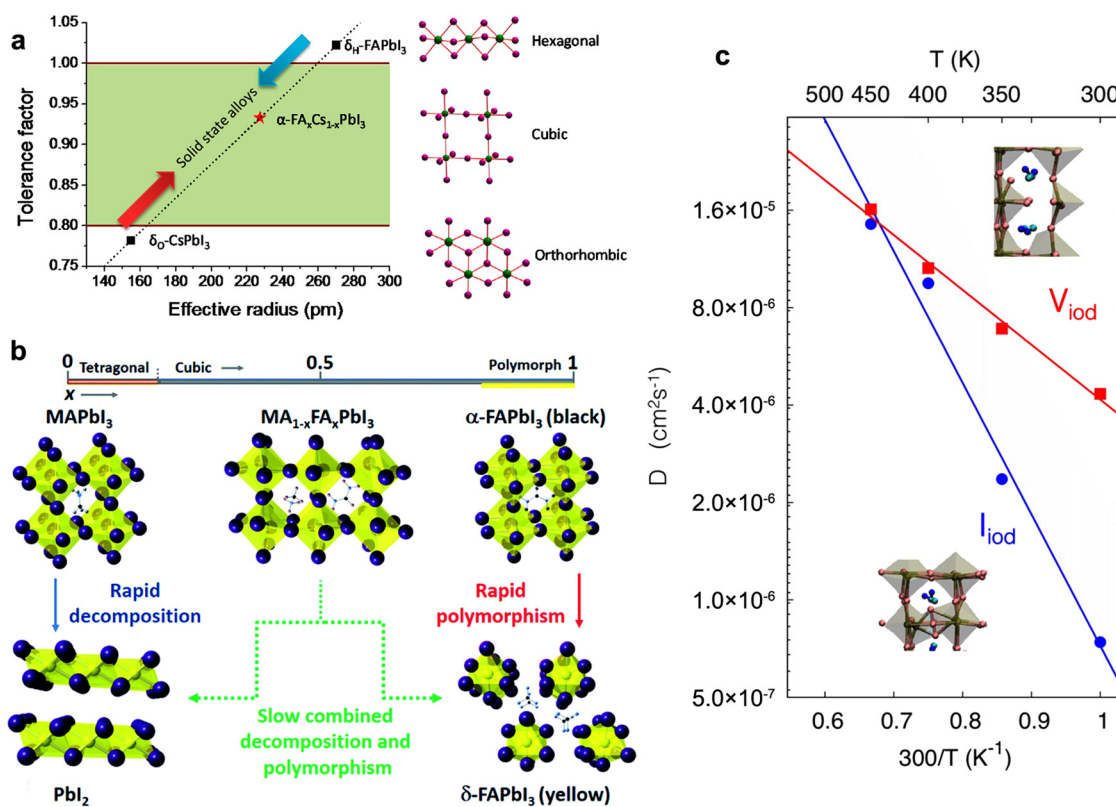


FIG. 9. (a) Tolerance factor determines the crystal structure of perovskites.¹⁴⁷ Reproduced with permission from Li *et al.*, Chem. Mater. **28**, 284 (2016). Copyright 2016 ACS Publications. (b) Cation mixing to avoid either polymorphism or decomposition.⁵⁸ Charles *et al.*, J. Mater. Chem. A **5**, 22495 (2017). Copyright 2017 Author(s), licensed under a Creative Commons Attribution (CC BY) license. (c) The mean square displacements (top, V_I and bottom, I_I) obtained by finite-temperature MD simulations.¹²⁷ Reproduced with permission from Delugas *et al.*, J. Phys. Chem. Lett. **7**, 2356 (2016). Copyright 2016 ACS Publications.

defects suppression and operational stability enhancement of perovskite based photovoltaics.^{151–160}

During the operation of perovskite solar cells, a great deal of defects is evolved to deteriorate the photovoltaic performance. Typically, ion migration under electric field could bring out a lot of vacancies and interstitials as discussed above. The chemical instability of perovskites under various aging stresses also allow the generation of many defects like Pb^0 and I^0 . These defects serve as not only recombination centers to deteriorate device efficiency but also degradation initiators to hamper device lifetimes. Our group innovatively incorporate the europium ion pair (Eu^{3+} - Eu^{2+}) into perovskite absorber, which becomes the “redox shuttle” to effectively and simultaneously suppress the Pb^0 and I^0 defects [Fig. 10(a)].¹⁵¹ Eu^{3+}

could selectively oxidize Pb^0 to Pb^{2+} and the formed Eu^{2+} selectively reduces I^0 to I^- . As a consequence, the concentration of Pb^0 and I^0 defects has reduced by an order of magnitude. Furthermore, with the redox shuttle incorporated, the resultant devices without any encapsulation maintained 90% of the original efficiency after 8000 h storage, 92% of the original efficiency after 1-sun continuous illumination for 1500 h, 89% after thermal aging at 85 °C for 1500 h, and 91% of the original stable efficiency after MPP tracking for 500 h, respectively [Fig. 10(b)]. In addition, halide anion and organic cation vacancies are the other two ubiquitous defects, which lead to thin-film decomposition at surfaces and grain boundaries. Our group then employ fluoride to simultaneously passivate both anion and cation vacancies in FAMACs mixed halide

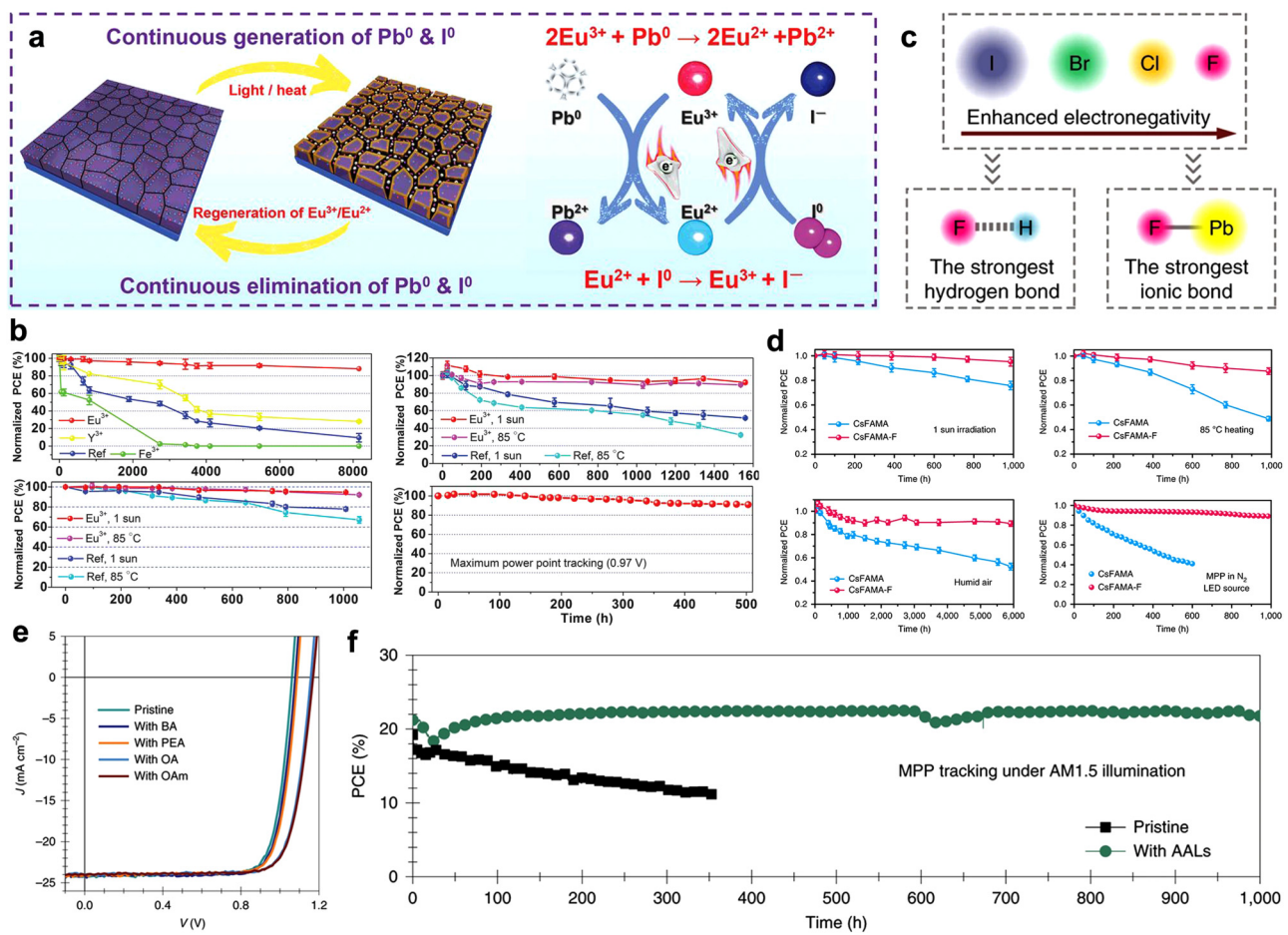


FIG. 10. (a) Proposed mechanism diagram of cyclical elimination of Pb^0 and I^0 defects and regeneration of Eu^{3+} - Eu^{2+} metal ion pair.¹⁵¹ Reproduced with permission from Wang *et al.*, Science **363**, 265 (2019). Copyright 2019 AAAS. (c) Schematic illustration of enhancing hydrogen bond and ionic bond by increasing the electronegativity of halogen.¹⁵² Reproduced with permission from Li *et al.*, Nat. Energy **4**, 408 (2019). Copyright 2019 Nature Publishing Group. (e) J - V characteristics of CsFAMA devices with the addition of AALs with different alkyl-chain lengths. (f) 1000 h of continuous MPP tracking for the pristine and AAL modified devices under simulated solar illumination (100 mW cm^{-2}) in a nitrogen atmosphere with a UV filter with a 420-nm cutoff.¹⁵⁴ Reproduced with permission from Zheng *et al.*, Nat. Energy **5**, 131 (2020). Copyright 2020 Nature Publishing Group.

perovskites, and theoretical calculation suggests that the fluoride ion could suppress the formation of both V_I and V_{FA} , through a unique strengthening of the ion bond with surrounding Pb cations, and the hydrogen bond with FA/MA cations, which originated from the extremely high electronegativity of fluoride [Fig. 10(c)].¹⁵² Besides, fluoride introduced devices exhibited obviously improved stability in various aging stresses of humid air, 1 sun illumination, 85 °C heating, and MPP operation. Particularly, the optimized solar cells without encapsulation retain 90% of its original efficiency after 1000 h of operation at MPP [Fig. 10(d)]. Moreover, Zheng *et al.* declare that oleylamine and octylamine with long-alkyl chain could suppress defects directly through filling in A-site vacancies and promote favorable grain orientation to further anchor the surface defects in perovskite absorber [Fig. 10(e)].¹⁵⁴ With such optimization, the p-i-n devices could continuously operate over 1000 h at MPP under simulated AM 1.5 illumination, without loss of efficiency [Fig. 10(f)].

In addition to the careful manipulation of defects, the suppression of ion migration in perovskite absorbers, especially under illumination and heating, also dramatically help to improve the

stability of resulting devices. Recently, Bai *et al.* incorporate a novel ionic liquid (1-butyl-3-methylimidazolium tetrafluoroborate, named BMIMBF₄) into perovskite absorber to effectively mitigate the ion migration. A clear luminescence quenching difference from the positive toward the negative electrode for the control and BMIMBF₄ films is observed [Fig. 11(a)].¹⁵³ This strategy remarkably improves the long-term stability of p-i-n planar perovskite solar cells. Specifically, only around 5% degradation of performance is observed in the most stable encapsulated device, which ages more than 1800 h under continuous simulated illumination and thermal aging of 75 °C. In addition, the estimated lifetime to 80% of original efficiency (T_{80}) is about 5200 h [Fig. 11(b)]. Moreover, Tan *et al.* investigate the effect of size-mismatch-induced lattice distortions on the ion migration and operational stability of perovskite solar cells. Acetamidinium is introduced to mismatch the size of “A” site composition and impede the migration pathways of ions by a steric effect [Fig. 11(c)].¹²⁸ Consequently, the optimized devices exhibit greatly improved thermal stability under aging at 85 °C and operational stability under continuous 1-sun illumination, with an extrapolated T_{80} lifetime of 2011 h [Fig. 11(d)].

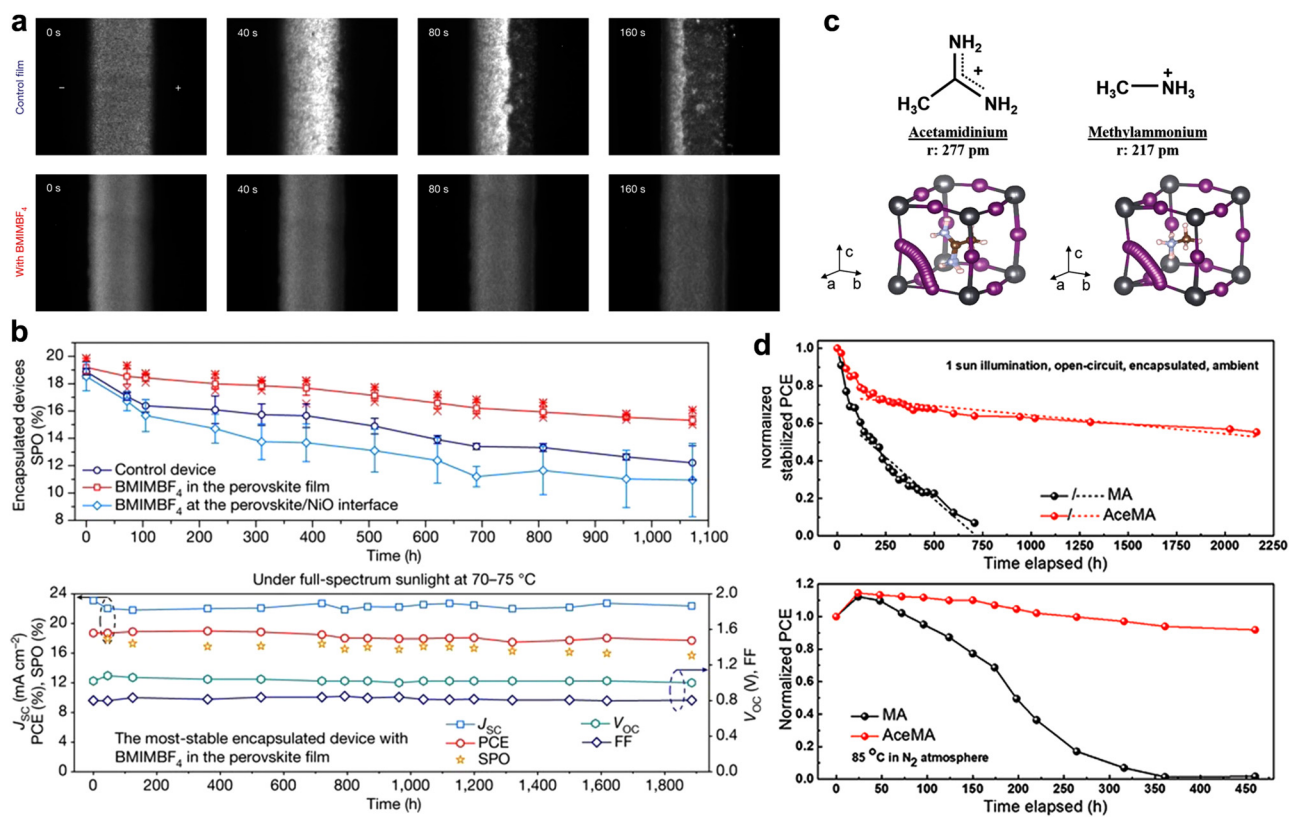


FIG. 11. (a) Photoluminescence images of control film and BMIMBF₄-containing film under a constant applied bias (10 V). The bright areas represent PL emission from the perovskite films.¹⁵³ Reproduced with permission from Bai *et al.*, *Nature* **571**, 245 (2019). Copyright 2019 Nature Publishing Group. (c) Chemical structures of acetamidinium, methylammonium, and DFT modeled side view iodide ion migration pathway. (d) Operational and thermal stability testing of the MAPbI₃ and Ace_{0.03}MA_{0.97}PbI₃ devices.¹²⁸ Reproduced with permission from Tan *et al.*, *Adv. Mater.* **32**, 1906995 (2020). Copyright 2020 Wiley-VCH.

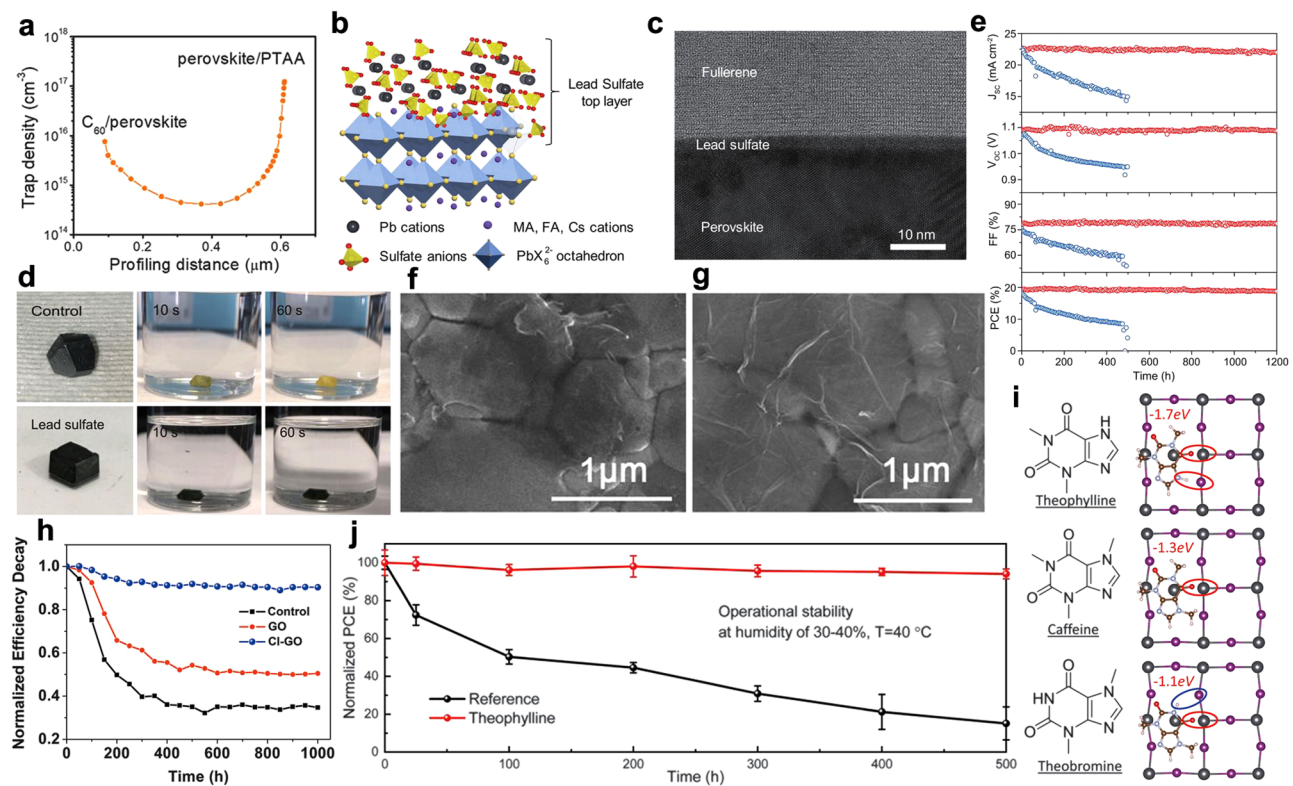


FIG. 12. (a) Dependence of the trap density on the profiling distance for the perovskite thin film in solar cells.⁵¹ Reproduced with permission from Ni *et al.*, Science 367, 1352 (2020). Copyright 2020 AAAS. (b) Schematic illustration of protection of perovskites through *in situ* formation of a PbSO₄ top layer. (c) Cross-sectional HR-TEM image of the perovskite/PbSO₄/C60 interface. (d) MAPbI₃ single crystals without and with PbSO₄ top layers dipped into water at different time intervals.¹⁵⁶ Reproduced with permission from Yang *et al.*, Science 365, 473 (2019). Copyright 2019 AAAS. (f) and (g) SEM images of perovskite/GO and perovskite/Cl-GO. (h) Operational stability of control cell and the cell with GO or Cl-GO.¹⁵⁹ Reproduced with permission from Wang *et al.*, Science 365, 687 (2019). Copyright 2019 AAAS. (i) Theoretical models of perovskite with molecular surface passivation of Pb_I antisite with theophylline, caffeine, and theobromine. (j) Evolution of efficiencies measured under open-circuit condition from encapsulated perovskite solar cells with or without theophylline treatment exposed to continuous light.¹⁶⁰ Reproduced with permission from Wang *et al.*, Science 366, 1509 (2019). Copyright 2019 AAAS.

Furthermore, many recent developed strategies with regard to interface modification also significantly improve the long-term stability of perovskite photovoltaics. Ni *et al.* have experimentally profiled the spatial and energetic distributions of defect states in polycrystalline perovskite solar cells and found the charge defect density at the interfaces is one to two orders of magnitude greater than that of the film interior [Fig. 12(a)].⁵¹ Yang *et al.* present the converting the surface of perovskite films to lead (II) oxysalt (PbSO₄) through the chemical reaction with sulfate ions, which effectively improve the water resistance of the perovskite films by forming strong chemical bonds and stabilize the interface between perovskites and hole transport layers via passivating undercoordinated surface lead centers and reducing the defect density [Figs. 12(b)–12(d)].¹⁵⁸ The encapsulated devices stabilized by the PbSO₄ layer maintain 96.8% of initial efficiency after continuous operation at MPP under simulated AM 1.5G irradiation for 1200 h at 65 °C [Fig. 12(e)]. Besides, a chlorinated graphene oxide (Cl-GO) is also introduced to stabilize the Pb-rich interface of perovskite-based heterostructure through strong Pb–Cl and Pb–O bonds [Figs. 12(f) and 12(g)]. The perovskite/Cl-GO

heterostructure could effectively impede the loss of decomposed components from soft perovskite absorbers, thus improving the stability of the corresponding photovoltaic devices. The encapsulated devices with perovskite/Cl-GO heterostructure kept 90% of their original efficiency of 21% after operation at MPP under AM 1.5G solar light at 60 °C for 1000 h [Fig. 12(h)].¹⁵⁹ Moreover, theophylline, caffeine, and theobromine with the same functional group are investigated to activate the defects passivation. The authors found the formation of hydrogen bond between N–H and I (iodine) assists the C=O binding [Fig. 12(i)] with the anti-site Pb–I defects to maximize defects anchoring at interface. The optimized device with encapsulation retained >90% of its initial efficiency when exposed to continuous illumination under open-circuit condition for ~500 h [Fig. 12(j)].¹⁶⁰

VI. SUMMARY AND OUTLOOK

Hybrid halide perovskite based photovoltaic techniques have been developed for just about 10 years, which has achieved a

skyrocketing power conversion efficiency of 25.2% (certified). The rapid development partially relies on the in-depth understanding of defects evolution and relevant suppression strategies. Nowadays, critical issues with regard to the long-term operational stability gradually emerge to impede further commercialization of perovskite solar cells. The long-term stability of devices is influenced by many factors including materials compositions, device structures, transport layers, and the interfaces. As the perovskite absorber itself is indispensable, their chemical stability is vital to device lifetime, wherein varieties of defects responsible for complex degradation pathways deteriorate materials stability in a fast and irreversible manner.

In this review, we have provided an in-depth discussion to understand defects chemistry in perovskite films and devices with the focus on the origin and influence of various defects and to underline the predominant role of defects at grain boundaries and surfaces. Moreover, we highlight reduction of defect-assisted non-radiative recombination at the interfaces relevant to perovskite is the effective strategy to further improve the efficiency of perovskite solar cells to reach the Shockley–Queisser limit. Additionally, we review the defects induced degradation process involving ion migration, moisture, oxygen, irradiation, and thermal stress. Defects within perovskite absorbers, in particular, at the grain boundaries and surfaces, always serve as the degradation initiators during the long-term operation to deteriorate photovoltaic performance. The careful management and even repair of the defects are necessary to effectively alleviate different degradation such as the phase segregation, the chemical reaction, and ion migration. Thus, we further review the recent significant strategies aiming at the defects suppression and long-term stability improvement for perovskite solar cells.

In viewing the recent progress in perovskite solar cells, it yet lacks a clear understanding on defects and its evolution in perovskite absorbers, especially during device operation. It is mostly due to the fragile nature of hybrid halide perovskites, wherein high resolution characterization techniques feasible for other materials do not work well. To further improve their operational stability and efficiency of halide perovskite solar cells, we briefly discuss a few challenges in the context of defect chemistry, which suggests the future research direction of interest.

A. Defects formation mechanisms and modulation strategies

The formation of defect states in perovskite absorbers is strongly influenced by the preparation process. To date, a lot of strategies focus on different fabrication technology, wherein various additives employment have been developed to decrease the defects density and suppress the non-radiative recombination centers successfully. However, most efforts emphasize the effects on reduction of defects concentration, while the deep connections between defects formation and preparation methods are still unclear. Therefore, it is a great challenge to double-check the defect states in perovskite films from a chemistry viewpoint ingeniously. In particular, the investigation must step beyond defects density to detail the species characteristics and their origins. In this respect, we suggest that two aspects may worth future efforts. First, the perovskite single crystals provide

a more reliable platform to study the defect states as compared to thin films because of their natively low defect density and simple defect environment. Moreover, it is easy to manipulate some material properties in single crystals, such as exposure of certain crystallographic planes, which may offer straightforward guidance for the development of perovskite thin film growth, and even single crystal solar cells fabrication. Second, polycrystalline perovskite absorber reveals relatively complicated defect environment due to the existence of numerous grain boundaries. The modulation of defects may further utilize the reactive nature of perovskite to suppress defects effectively by leveraging the established chemical approach. For example, interstitial I defects commonly exist in iodine-based perovskites, which serve as non-radiative recombination centers. The iodine disproportionation chemistry reaction was involved to eliminate these defects effectively, not only in thin films but also in precursors.^{29,38,45} Future research studies can refer to more chemistry reactions in the fabrication process of perovskites to optimize the defect states in resultant absorbers.

B. Surface defects passivation mechanism

The passivation of defect states at surfaces and grain boundaries plays a vital role in the evolution of both efficiency and stability for perovskite solar cells as mentioned above. However, a complete understanding of passivation mechanism for different passivators, namely, the interaction between passivators and surface defects, have not been totally resolved. This issue becomes even complex when mixed perovskite absorbers are popularly adopted via diversity of preparation methods and addition of various multifunctional additives. It is essential to uncover the underlying working mechanism of passivators in a clear environment, which could guide the passivator design and method adjustment effectively in the future. For example, in the scenario of charged defects at the surface of perovskite films, the unique passivator with both negatively and positively charged centers was designed to simultaneously passivate the positively and negatively charged defects at the surface of perovskite films by the coulomb interactions.¹⁰⁴ The strong chemical ion bonds were formed by introducing lead oxysalt thin layers at the surface of perovskites and thus passivated the undercoordinated lead defects at surface. In this respect, future investigations might focus on the formation of stronger covalent bonds at the surface of perovskite, borrowing a similar idea in silicon solar cells, where SiO_2 and Si_3N_4 successfully passivate the dangling bonds at wafer surface. Combined with the controllable formation and modulation of defects in the perovskite absorber, the followed and refined surface defects passivation is the straight pathway toward the improved efficiency approaching Shockley–Queisser theoretic limit.

C. Defects evolution and degradation pathway of perovskite devices

The poor long-term operational stability is a key problem restricting the rapid development of perovskite photovoltaics for practical use. As we discussed above, predominant defects trigger most degradation processes of perovskite devices under different aging stresses to take irreversible effects. Specifically, the accumulation of new defect states will accelerate the complex aging processes,

which leads to even more defects. To break up this chain degradation, it is highly urgent to understand the defects evolution in perovskite films during different aging processes. As long as every stages in the efficiency degradation of perovskite solar cells are clearly described, specifically designed silver-bullets are hopefully to be available. For instance, the long-term operation of Pb-I perovskite solar cells under illumination will steadily generate I^0 and Pb^0 defects pair. A self-regenerated Eu^{3+} - Eu^{2+} ion redox shuttle was thus introduced to eliminate these defects pair simultaneously by involving the electron transfer process in a sustainable manner. Future studies can refer to the other major defects, which constantly arose during the long-term device operation, like the MA and I related vacancies due to its improved volatility. In addition, ion migration also introduced new defect states in perovskites continually, thus the management of ion migration is critical to inhibit the degradation of perovskite devices and improve the long-term operational stability. With this regard, fruitful results are expected by understanding defect evolution and degradation pathway.

ACKNOWLEDGMENTS

This work was supported by the National Natural Science Foundation of China (Nos. 51722201, 51672008, 51972004, and 91733301), National Key Research and Development Program of China (Grant No. 2017YFA0206701), and Natural Science Foundation of Beijing, China (Grant No. 4182026).

DATA AVAILABILITY

The data that support the findings of this study are available from the corresponding author upon reasonable request.

REFERENCES

- ¹M. A. Green, A. Ho-Baillie, and H. J. Snaith, *Nat. Photonics* **8**, 506 (2014).
- ²N.-G. Park, M. Grätzel, T. Miyasaka, K. Zhu, and K. Emery, *Nat. Energy* **1**, 16152 (2016).
- ³A. Kojima, K. Teshima, Y. Shirai, and T. Miyasaka, *J. Am. Chem. Soc.* **131**, 6050 (2009).
- ⁴A. Buin, R. Comin, J. Xu, A. H. Ip, and E. H. Sargent, *Chem. Mater.* **27**, 4405 (2015).
- ⁵G. E. Eperon, S. D. Stranks, C. Menelaou, M. B. Johnston, L. M. Herz, and H. J. Snaith, *Energy Environ. Sci.* **7**, 982 (2014).
- ⁶W. J. Yin, T. Shi, and Y. Yan, *Adv. Mater.* **26**, 4653 (2014).
- ⁷J. Huang, Y. Yuan, Y. Shao, and Y. Yan, *Nat. Rev. Mater.* **2**, 17042 (2017).
- ⁸C. Wehrenfennig, G. E. Eperon, M. B. Johnston, H. J. Snaith, and L. M. Herz, *Adv. Mater.* **26**, 1584 (2014).
- ⁹M. M. Lee, J. Teuscher, T. Miyasaka, T. N. Murakami, and H. J. Snaith, *Science* **338**, 643 (2012).
- ¹⁰M. Liu, M. B. Johnston, and H. J. Snaith, *Nature* **501**, 395 (2013).
- ¹¹K. Galkowski, A. Mitioglu, A. Miyata, P. Plochocka, O. Portugall, G. E. Eperon, J. T.-W. Wang, T. Stergiopoulos, S. D. Stranks, H. J. Snaith, and R. J. Nicholas, *Energy Environ. Sci.* **9**, 962 (2016).
- ¹²H. J. Snaith, *J. Phys. Chem. Lett.* **4**, 3623 (2013).
- ¹³J. Mizusaki, K. Arai, and K. Fueki, *Solid State Ionics* **11**, 203 (1983).
- ¹⁴D. Shi, V. Adinolfi, R. Comin, M. Yuan, E. Alarousu, A. Buin, Y. Chen, S. Hoogland, A. Rothenberger, and K. Katsiev, *Science* **347**, 519 (2015).
- ¹⁵S. G. Motti, D. Meggiolaro, S. Martani, R. Sorrentino, A. J. Barker, F. De Angelis, and A. Petrozza, *Adv. Mater.* **31**, 1901183 (2019).
- ¹⁶W.-J. Yin, T. Shi, and Y. Yan, *Appl. Phys. Lett.* **104**, 063903 (2014).
- ¹⁷C. Ran, J. Xu, W. Gao, C. Huang, and S. Dou, *Chem. Soc. Rev.* **47**, 4581 (2018).
- ¹⁸J. M. Ball and A. Petrozza, *Nat. Energy* **1**, 16149 (2016).
- ¹⁹J. Tong, Z. Song, D. H. Kim, X. Chen, C. Chen, A. F. Palmstrom, P. F. Ndione, M. O. Reese, S. P. Dunfield, O. G. Reid, J. Liu, F. Zhang, S. P. Harvey, Z. Li, S. T. Christensen, G. Teeter, D. Zhao, M. M. Al-Jassim, M. F. A. M. van Hest, M. C. Beard, S. E. Shaheen, J. J. Berry, Y. Yan, and K. Zhu, *Science* **364**, 475 (2019).
- ²⁰D. P. McMeekin, S. Mahesh, N. K. Noel, M. T. Klug, J. Lim, J. H. Warby, J. M. Ball, L. M. Herz, M. B. Johnston, and H. J. Snaith, *Joule* **3**, 1 (2019).
- ²¹R. Lin, K. Xiao, Z. Qin, Q. Han, C. Zhang, M. Wei, M. I. Saidaminov, Y. Gao, J. Xu, M. Xiao, A. Li, J. Zhu, E. H. Sargent, and H. Tan, *Nat. Energy* **4**, 864 (2019).
- ²²F. Sahli, J. Werner, B. A. Kamino, M. Braunerger, R. Monnard, B. Paviet-Salomon, L. Barraud, L. Ding, J. J. Diaz Leon, D. Sacchetto, G. Cattaneo, M. Despeisse, M. Boccard, S. Nicolay, Q. Jeangros, B. Niesen, and C. Ballif, *Nat. Mater.* **17**, 820 (2018).
- ²³J. Xu, C. C. Boyd, Z. J. Yu, A. F. Palmstrom, D. J. Witter, B. W. Larson, R. M. France, J. Werner, S. P. Harvey, E. J. Wolf, W. Weigand, S. Manzoor, M. F. A. M. van Hest, J. J. Berry, J. M. Luther, Z. C. Holman, and M. D. McGhee, *Science* **367**, 1097 (2020).
- ²⁴Z. Li, Y. Zhao, X. Wang, Y. Sun, Z. Zhao, Y. Li, H. Zhou, and Q. Chen, *Joule* **2**, 1559 (2018).
- ²⁵N. L. Chang, A. W. Yi Ho-Baillie, P. A. Basore, T. L. Young, R. Evans, and R. J. Egan, *Prog. Photovolt. Res. Appl.* **25**, 390 (2017).
- ²⁶Z. Song, C. L. McElvany, A. B. Phillips, I. Celik, P. W. Krantz, S. C. Watthage, G. K. Liyanage, D. Apul, and M. J. Heben, *Energy Environ. Sci.* **10**, 1297 (2017).
- ²⁷M. Cai, Y. Wu, H. Chen, X. Yang, Y. Qiang, and L. Han, *Adv. Sci.* **4**, 1600269 (2017).
- ²⁸Q. F. Dong, Y. J. Fang, Y. C. Shao, P. Mulligan, J. Qiu, L. Cao, and J. S. Huang, *Science* **347**, 967 (2015).
- ²⁹Y. Chen, N. Li, L. Wang, L. Li, Z. Xu, H. Jiao, P. Liu, C. Zhu, H. Zai, M. Sun, W. Zou, S. Zhang, G. Xing, X. Liu, J. Wang, D. Li, B. Huang, Q. Chen, and H. Zhou, *Nat. Commun.* **10**, 1112 (2019).
- ³⁰M. Saliba, T. Matsui, K. Domanski, J.-Y. Seo, A. Ummadisingu, S. M. Zakeeruddin, J.-P. Correa-Baena, W. R. Tress, A. Abate, and A. Hagfeldt, *Science* **354**, 206 (2016).
- ³¹K. T. Cho, S. Paek, G. Grancini, C. Roldán-Carmona, P. Gao, Y. Lee, and M. K. Nazeeruddin, *Energy Environ. Sci.* **10**, 621 (2017).
- ³²W. S. Yang, B. W. Park, E. H. Jung, N. J. Jeon, Y. C. Kim, D. U. Lee, S. S. Shin, J. Seo, E. K. Kim, J. H. Noh, and S. I. Seok, *Science* **356**, 1376 (2017).
- ³³G. Zheng, C. Zhu, J. Ma, X. Zhang, G. Tang, R. Li, Y. Chen, L. Li, J. Hu, J. Hong, Q. Chen, X. Gao, and H. Zhou, *Nat. Commun.* **9**, 2793 (2018).
- ³⁴G. Zheng, C. Zhu, Y. Chen, J. Zhang, Q. Chen, X. Gao, and H. Zhou, *Chem. Commun.* **53**, 12966 (2017).
- ³⁵D.-Y. Son, J.-W. Lee, Y. J. Choi, I.-H. Jang, S. Lee, P. J. Yoo, H. Shin, N. Ahn, M. Choi, D. Kim, and N.-G. Park, *Nat. Energy* **1**, 16081 (2016).
- ³⁶N. Ahn, D. Y. Son, I. H. Jang, S. M. Kang, M. Choi, and N. G. Park, *J. Am. Chem. Soc.* **137**, 8696 (2015).
- ³⁷L. Li, Y. Chen, Z. Liu, Q. Chen, X. Wang, and H. Zhou, *Adv. Mater.* **28**, 9862 (2016).
- ³⁸D. Zhang, B. B. Cui, C. Zhou, L. Li, Y. Chen, N. Zhou, Z. Xu, Y. Li, H. Zhou, and Q. Chen, *Chem. Commun.* **53**, 10548 (2017).
- ³⁹F. Gu, S. Ye, Z. Zhao, H. Rao, Z. Liu, Z. Bian, and C. Huang, *Sol. RRL* **2**, 1800136 (2018).
- ⁴⁰J. W. Lee, H. S. Kim, and N. G. Park, *Acc. Chem. Res.* **49**, 311 (2016).
- ⁴¹J.-W. Lee, S.-H. Bae, Y.-T. Hsieh, N. De Marco, M. Wang, P. Sun, and Y. Yang, *Chem* **3**, 290 (2017).
- ⁴²M. Kim, G.-H. Kim, T. K. Lee, I. W. Choi, H. W. Choi, Y. Jo, Y. J. Yoon, J. W. Kim, J. Lee, D. Huh, H. Lee, S. K. Kwak, Y. Kim, and D. S. Kim, *Joule* **3**, 1 (2019).
- ⁴³H. P. Zhou, Q. Chen, G. Li, S. Luo, T. B. Song, H. S. Duan, Z. R. Hong, J. B. You, Y. S. Liu, and Y. Yang, *Science* **345**, 542 (2014).

- ⁴⁴Z. Xiao, Q. Dong, C. Bi, Y. Shao, Y. Yuan, and J. Huang, *Adv. Mater.* **26**, 6503 (2014).
- ⁴⁵Z. Liu, J. Hu, H. Jiao, L. Li, G. Zheng, Y. Chen, Y. Huang, Q. Zhang, C. Shen, Q. Chen, and H. Zhou, *Adv. Mater.* **29**, 1606774 (2017).
- ⁴⁶S. Ye, H. Rao, Z. Zhao, L. Zhang, H. Bao, W. Sun, Y. Li, F. Gu, J. Wang, Z. Liu, Z. Bian, and C. Huang, *J. Am. Chem. Soc.* **139**, 7504 (2017).
- ⁴⁷Y. Shao, Z. Xiao, C. Bi, Y. Yuan, and J. Huang, *Nat. Commun.* **5**, 5784 (2014).
- ⁴⁸A. Baumann, S. Vath, P. Rieder, M. C. Heiber, K. Tvingstedt, and V. Dyakonov, *J. Phys. Chem. Lett.* **6**, 2350 (2015).
- ⁴⁹M. Stolterfoht, C. M. Wolff, J. A. Márquez, S. Zhang, C. J. Hages, D. Rothhardt, S. Albrecht, P. L. Burn, P. Meredith, T. Unold, and D. Neher, *Nat. Energy* **3**, 847 (2018).
- ⁵⁰V. Sarritzu, N. Sestu, D. Marongiu, X. Chang, S. Masi, A. Rizzo, S. Colella, F. Quochi, M. Saba, A. Mura, and G. Bongiovanni, *Sci. Rep.* **7**, 44629 (2017).
- ⁵¹Z. Ni, C. Bao, Y. Liu, Q. Jiang, W. Q. Wu, S. Chen, X. Dai, B. Chen, B. Hartweg, Z. Yu, Z. Holman, and J. Huang, *Science* **367**, 1352 (2020).
- ⁵²C. Boyd, R. Cheacharoen, T. Leijtens, and M. D. McGehee, *Chem. Rev.* **119**, 3418 (2019).
- ⁵³T. A. Berhe, W.-N. Su, C.-H. Chen, C.-J. Pan, J.-H. Cheng, H.-M. Chen, M.-C. Tsai, L.-Y. Chen, A. A. Dubale, and B.-J. Hwang, *Energy Environ. Sci.* **9**, 323 (2016).
- ⁵⁴Z. Qiu, N. Li, Z. Huang, Q. Chen, and H. Zhou, *Small Methods* **4**, 1900877 (2020).
- ⁵⁵J. Yang, B. D. Siempelkamp, E. Mosconi, F. De Angelis, and T. L. Kelly, *Chem. Mater.* **27**, 4229 (2015).
- ⁵⁶N. J. Jeon, H. Na, E. H. Jung, T.-Y. Yang, Y. G. Lee, G. Kim, H.-W. Shin, S. Il Seok, J. Lee, and J. Seo, *Nat. Energy* **3**, 682 (2018).
- ⁵⁷D. Bryant, N. Aristidou, S. Pont, I. Sanchez-Molina, T. Chotchunangatchaval, S. Wheeler, J. R. Durrant, and S. A. Haque, *Energy Environ. Sci.* **9**, 1655 (2016).
- ⁵⁸B. Charles, J. Dillon, O. J. Weber, M. S. Islam, and M. T. Weller, *J. Mater. Chem. A* **5**, 22495 (2017).
- ⁵⁹N. Phung and A. Abate, *Small* **14**, 1802573 (2018).
- ⁶⁰L. Liu, S. Huang, Y. Lu, P. Liu, Y. Zhao, C. Shi, S. Zhang, J. Wu, H. Zhong, M. Sui, H. Zhou, H. Jin, Y. Li, and Q. Chen, *Adv. Mater.* **30**, 1800544 (2018).
- ⁶¹H. Huang, M. I. Bodnarchuk, S. V. Kershaw, M. V. Kovalenko, and A. L. Rogach, *ACS Energy Lett.* **2**, 2071 (2017).
- ⁶²B. Chen, P. N. Rudd, S. Yang, Y. Yuan, and J. Huang, *Chem. Soc. Rev.* **48**, 3842 (2019).
- ⁶³D. Yang, W. Ming, H. Shi, L. Zhang, and M.-H. Du, *Chem. Mater.* **28**, 4349 (2016).
- ⁶⁴N. Aristidou, C. Eames, I. Sanchez-Molina, X. Bu, J. Kosco, M. S. Islam, and S. A. Haque, *Nat. Commun.* **8**, 15218 (2017).
- ⁶⁵S.-H. Turren-Cruz, A. Hagfeldt, and M. Saliba, *Science* **362**, 449 (2018).
- ⁶⁶N. J. Jeon, J. H. Noh, W. S. Yang, Y. C. Kim, S. Ryu, J. Seo, and S. I. Seok, *Nature* **517**, 476 (2015).
- ⁶⁷E. H. Jung, N. J. Jeon, E. Y. Park, C. S. Moon, T. J. Shin, T. Y. Yang, J. H. Noh, and J. Seo, *Nature* **567**, 511 (2019).
- ⁶⁸M. Kim, S. G. Motti, R. Sorrentino, and A. Petrozza, *Energy Environ. Sci.* **11**, 2609 (2018).
- ⁶⁹G. Grancini, C. Roldan-Carmona, I. Zimmermann, E. Mosconi, X. Lee, D. Martineau, S. Narbey, F. Oswald, F. De Angelis, M. Graetzel, and M. K. Nazeeruddin, *Nat. Commun.* **8**, 15684 (2017).
- ⁷⁰F. Bella, G. Griffini, J.-P. Correa-Baena, G. Saracco, M. Grätzel, A. Hagfeldt, S. Turri, and C. Gerbaldo, *Science* **354**, 203 (2016).
- ⁷¹K. A. Bush, A. F. Palmstrom, Z. J. Yu, M. Boccard, R. Cheacharoen, J. P. Mailoa, D. P. McMeekin, R. L. Z. Hoye, C. D. Bailie, T. Leijtens, I. M. Peters, M. C. Minichetti, N. Rolston, R. Prasanna, S. Sofia, D. Harwood, W. Ma, F. Moghadam, H. J. Snaith, T. Buonassisi, Z. C. Holman, S. F. Bent, and M. D. McGehee, *Nat. Energy* **2**, 17009 (2017).
- ⁷²R. Prasanna, T. Leijtens, S. P. Dunfield, J. A. Raiford, E. J. Wolf, S. A. Swifter, J. Werner, G. E. Eperon, C. de Paula, A. F. Palmstrom, C. C. Boyd, M. F. A. M. van Hest, S. F. Bent, G. Teeter, J. J. Berry, and M. D. McGehee, *Nat. Energy* **4**, 939 (2019).
- ⁷³A. Walsh and A. Zunger, *Nat. Mater.* **16**, 964 (2017).
- ⁷⁴J. S. Park, S. Kim, Z. Xie, and A. Walsh, *Nat. Rev. Mater.* **3**, 194 (2018).
- ⁷⁵H. J. Queisser and E. E. Haller, *Science* **281**, 945 (1998).
- ⁷⁶A. Stoneham, *Theory of Defects in Solids* (Oxford University Press, Oxford, 1975).
- ⁷⁷Frenkel, *Z. Phys.* **35**, 652 (1926).
- ⁷⁸C. Freysoldt, B. Grabowski, T. Hickel, J. Neugebauer, G. Kresse, A. Janotti, and C. G. Van de Walle, *Rev. Mod. Phys.* **86**, 253 (2014).
- ⁷⁹D. Meggiolaro and F. De Angelis, *ACS Energy Lett.* **3**, 2206 (2018).
- ⁸⁰N. Liu and C. Yam, *Phys. Chem. Chem. Phys.* **20**, 6800 (2018).
- ⁸¹Y. Li, C. Zhang, X. Zhang, D. Huang, Q. Shen, Y. Cheng, and W. Huang, *Appl. Phys. Lett.* **111**, 162106 (2017).
- ⁸²Y. Huang, W.-J. Yin, and Y. He, *J. Phys. Chem. C* **122**, 1345 (2018).
- ⁸³S. P. Dunfield, L. Bliss, F. Zhang, J. M. Luther, K. Zhu, M. F. A. M. Hest, M. O. Reese, and J. J. Berry, *Adv. Energy Mater.* **0**, 1904054 (2020).
- ⁸⁴J. Kang and L. W. Wang, *J. Phys. Chem. Lett.* **8**, 489 (2017).
- ⁸⁵P. Xu, S. Chen, H.-J. Xiang, X.-G. Gong, and S.-H. Wei, *Chem. Mater.* **26**, 6068 (2014).
- ⁸⁶D. Meggiolaro, S. G. Motti, E. Mosconi, A. J. Barker, J. Ball, C. Andrea Riccardo Perini, F. Deschler, A. Petrozza, and F. De Angelis, *Energy Environ. Sci.* **11**, 702 (2018).
- ⁸⁷T. Shi, H.-S. Zhang, W. Meng, Q. Teng, M. Liu, X. Yang, Y. Yan, H.-L. Yip, and Y.-J. Zhao, *J. Mater. Chem. A* **5**, 15124 (2017).
- ⁸⁸T. S. Sherkar, C. Momblona, L. Gil-Escríg, J. Avila, M. Sessolo, H. J. Bolink, and L. J. A. Koster, *ACS Energy Lett.* **2**, 1214 (2017).
- ⁸⁹D. Meggiolaro, E. Mosconi, and F. De Angelis, *ACS Energy Lett.* **4**, 779 (2019).
- ⁹⁰M. L. Agiorgousis, Y. Y. Sun, H. Zeng, and S. Zhang, *J. Am. Chem. Soc.* **136**, 14570 (2014).
- ⁹¹A. Buin, P. Pietsch, J. Xu, O. Voznyy, A. H. Ip, R. Comin, and E. H. Sargent, *Nano Lett.* **14**, 6281 (2014).
- ⁹²D. Meggiolaro, E. Mosconi, and F. De Angelis, *ACS Energy Lett.* **3**, 447 (2018).
- ⁹³T. A. S. Doherty, A. J. Winchester, S. Macpherson, D. N. Johnstone, V. Pareek, E. M. Tennyson, S. Kosar, F. U. Kosasih, M. Anaya, M. Abdi-Jalebi, Z. Andaji-Garmaroudi, E. L. Wong, J. Madeo, Y. H. Chiang, J. S. Park, Y. K. Jung, C. E. Petoukhoff, G. Divitini, M. K. L. Man, C. Ducati, A. Walsh, P. A. Midgley, K. M. Dani, and S. D. Stranks, *Nature* **580**, 360 (2020).
- ⁹⁴J. Chen and N. G. Park, *Adv. Mater.* **31**, 1803019 (2019).
- ⁹⁵D. W. deQuilettes, K. Frohma, D. Emin, T. Kirchartz, V. Bulovic, D. S. Ginger, and S. D. Stranks, *Chem. Rev.* **119**, 11007 (2019).
- ⁹⁶W. Tress, M. Yavari, K. Domanski, P. Yadav, B. Niesen, J. P. Correa Baena, A. Hagfeldt, and M. Graetzel, *Energy Environ. Sci.* **11**, 151 (2018).
- ⁹⁷D. Luo, R. Su, W. Zhang, Q. Gong, and R. Zhu, *Nat. Rev. Mater.* **5**, 44 (2019).
- ⁹⁸L. M. Pazos-Outon, T. P. Xiao, and E. Yablonovitch, *J. Phys. Chem. Lett.* **9**, 1703 (2018).
- ⁹⁹D. Bi, W. Tress, M. I. Dar, P. Gao, J. Luo, C. Renevier, K. Schenk, A. Abate, F. Giordano, J.-P. C. Baena, J.-D. Decoppet, S. M. Zakeeruddin, M. K. Nazeeruddin, M. Grätzel, and A. Hagfeldt, *Sci. Adv.* **2**, 1501170 (2016).
- ¹⁰⁰C. M. Wolff, P. Caprioglio, M. Stolterfoht, and D. Neher, *Adv. Mater.* **31**, 1902762 (2019).
- ¹⁰¹Q. Jiang, Y. Zhao, X. Zhang, X. Yang, Y. Chen, Z. Chu, Q. Ye, X. Li, Z. Yin, and J. You, *Nat. Photonics* **13**, 460 (2019).
- ¹⁰²H. Zhu, Y. Liu, F. T. Eickemeyer, L. Pan, D. Ren, M. A. Ruiz-Preciado, B. Carlsen, B. Yang, X. Dong, Z. Wang, H. Liu, S. Wang, S. M. Zakeeruddin, A. Hagfeldt, M. I. Dar, X. Li, and M. Grätzel, *Adv. Mater.* **32**, 1907757 (2020).
- ¹⁰³J. J. Yoo, S. Wieghold, M. C. Sponseller, M. R. Chua, S. N. Bertram, N. T. P. Hartono, J. S. Tresback, E. C. Hansen, J.-P. Correa-Baena, V. Bulović, T. Buonassisi, S. S. Shin, and M. G. Bawendi, *Energy Environ. Sci.* **12**, 2192 (2019).
- ¹⁰⁴X. Zheng, B. Chen, J. Dai, Y. Fang, Y. Bai, Y. Lin, H. Wei, X. Zeng, and J. Huang, *Nat. Energy* **2**, 17102 (2017).
- ¹⁰⁵Q. Wang, B. Chen, Y. Liu, Y. Deng, Y. Bai, Q. Dong, and J. Huang, *Energy Environ. Sci.* **10**, 516 (2017).

- ¹⁰⁶Y. Ouyang, L. Shi, Q. Li, and J. Wang, *Small Methods* **3**, 1900154 (2019).
- ¹⁰⁷A. M. A. Leguy, Y. Hu, M. Campoy-Quiles, M. I. Alonso, O. J. Weber, P. Azarhoosh, M. van Schilfgaarde, M. T. Weller, T. Bein, J. Nelson, P. Docampo, and P. R. F. Barnes, *Chem. Mater.* **27**, 3397 (2015).
- ¹⁰⁸J. A. Christians, P. A. Miranda Herrera, and P. V. Kamat, *J. Am. Chem. Soc.* **137**, 1530 (2015).
- ¹⁰⁹A. J. Pearson, G. E. Eperon, P. E. Hopkinson, S. N. Habisreutinger, J. T.-W. Wang, H. J. Snaith, and N. C. Greenham, *Adv. Energy Mater.* **6**, 1600014 (2016).
- ¹¹⁰E. Mosconi, D. Meggiolaro, H. J. Snaith, S. D. Stranks, and F. De Angelis, *Energy Environ. Sci.* **9**, 3180 (2016).
- ¹¹¹Y. Shao, Y. Fang, T. Li, Q. Wang, Q. Dong, Y. Deng, Y. Yuan, H. Wei, M. Wang, A. Gruverman, J. Shield, and J. Huang, *Energy Environ. Sci.* **9**, 1752 (2016).
- ¹¹²Z. Li, C. Xiao, Y. Yang, S. P. Harvey, D. H. Kim, J. A. Christians, M. Yang, P. Schulz, S. U. Nanayakkara, C.-S. Jiang, J. M. Luther, J. J. Berry, M. C. Beard, M. M. Al-Jassim, and K. Zhu, *Energy Environ. Sci.* **10**, 1234 (2017).
- ¹¹³J. Haruyama, K. Sodeyama, L. Han, and Y. Tateyama, *J. Am. Chem. Soc.* **137**, 10048 (2015).
- ¹¹⁴J. Chen, D. Lee, and N. G. Park, *ACS Appl. Mater. Interfaces* **9**, 36338 (2017).
- ¹¹⁵H. J. Snaith, A. Abate, J. M. Ball, G. E. Eperon, T. Leijtens, N. K. Noel, S. D. Stranks, J. T. Wang, K. Wojciechowski, and W. Zhang, *J. Phys. Chem. Lett.* **5**, 1511 (2014).
- ¹¹⁶P. Calado, A. M. Telford, D. Bryant, X. Li, J. Nelson, B. C. O'Regan, and P. R. Barnes, *Nat. Commun.* **7**, 13831 (2016).
- ¹¹⁷D. Y. Son, S. G. Kim, J. Y. Seo, S. H. Lee, H. Shin, D. Lee, and N. G. Park, *J. Am. Chem. Soc.* **140**, 1358 (2018).
- ¹¹⁸Y. Yuan, T. Li, Q. Wang, J. Xing, A. Gruverman, and J. Huang, *Sci. Adv.* **3**, 1602164 (2017).
- ¹¹⁹E. Juarez-Perez, R. S. Sanchez, L. Badia, G. Garcia-Belmonte, Y. S. Kang, I. Mora-Sero, and J. Bisquert, *J. Phys. Chem. Lett.* **5**, 2390 (2014).
- ¹²⁰X. Tang, M. van den Berg, E. Gu, A. Horneber, G. J. Matt, A. Osvet, A. J. Meixner, D. Zhang, and C. J. Brabec, *Nano Lett.* **18**, 2172 (2018).
- ¹²¹S. J. Yoon, M. Kuno, and P. V. Kamat, *ACS Energy Lett.* **2**, 1507 (2017).
- ¹²²I. M. Hermes, Y. Hou, V. W. Bergmann, C. J. Brabec, and S. A. L. Weber, *J. Phys. Chem. Lett.* **9**, 6249 (2018).
- ¹²³J. Carrillo, A. Guerrero, S. Rahimnejad, O. Almora, I. Zarazua, E. Mas-Marza, J. Bisquert, and G. Garcia-Belmonte, *Adv. Energy Mater.* **6**, 1502246 (2016).
- ¹²⁴C. Eames, J. M. Frost, P. R. Barnes, B. C. O'Regan, A. Walsh, and M. S. Islam, *Nat. Commun.* **6**, 7497 (2015).
- ¹²⁵Y. Yuan and J. Huang, *Acc. Chem. Res.* **49**, 286 (2016).
- ¹²⁶J. M. Azpiroz, E. Mosconi, J. Bisquert, and F. De Angelis, *Energy Environ. Sci.* **8**, 2118 (2015).
- ¹²⁷P. Delugas, C. Caddeo, A. Filippetti, and A. Mattoni, *J. Phys. Chem. Lett.* **7**, 2356 (2016).
- ¹²⁸S. Tan, I. Yavuz, N. De Marco, T. Huang, S. J. Lee, C. S. Choi, M. Wang, S. Nuryyeva, R. Wang, Y. Zhao, H. C. Wang, T. H. Han, B. Dunn, Y. Huang, J. W. Lee, and Y. Yang, *Adv. Mater.* **32**, 1906995 (2020).
- ¹²⁹X. Xiao, J. Dai, Y. Fang, J. Zhao, X. Zheng, S. Tang, P. N. Rudd, X. C. Zeng, and J. Huang, *ACS Energy Lett.* **3**, 684 (2018).
- ¹³⁰D. A. Egger, L. Kronik, and A. M. Rappe, *Angew. Chem. Int. Ed. Engl.* **54**, 12437 (2015).
- ¹³¹N. Phung, A. Al-Ashouri, S. Meloni, A. Mattoni, S. Albrecht, E. L. Unger, A. Merdasa, and A. Abate, *Adv. Energy Mater.* **10**, 1903735 (2020).
- ¹³²S. A. L. Weber, I. M. Hermes, S.-H. Turren-Cruz, C. Gort, V. W. Bergmann, L. Gilson, A. Hagfeldt, M. Graetzel, W. Tress, and R. Berger, *Energy Environ. Sci.* **11**, 2404 (2018).
- ¹³³C. Caddeo, A. Filippetti, and A. Mattoni, *Nano Energy* **67**, 104162 (2020).
- ¹³⁴L. Ling, S. Yuan, P. Wang, H. Zhang, L. Tu, J. Wang, Y. Zhan, and L. Zheng, *Adv. Funct. Mater.* **26**, 5028 (2016).
- ¹³⁵N. Ahn, K. Kwak, M. S. Jang, H. Yoon, B. Y. Lee, J. K. Lee, P. V. Pikhitsa, J. Byun, and M. Choi, *Nat. Commun.* **7**, 13422 (2016).
- ¹³⁶N. Aristidou, I. Sanchez-Molina, T. Chotchuangchutchaval, M. Brown, L. Martinez, T. Rath, and S. A. Haque, *Angew. Chem. Int. Ed. Engl.* **54**, 8208 (2015).
- ¹³⁷E. Carter, A. F. Carley, and D. M. Murphy, *J. Phys. Chem. C* **111**, 10630 (2007).
- ¹³⁸T. Leijtens, G. E. Eperon, S. Pathak, A. Abate, M. M. Lee, and H. J. Snaith, *Nat. Commun.* **4**, 2885 (2013).
- ¹³⁹Y. Li, J. K. Cooper, W. Liu, C. M. Sutter-Fella, M. Amani, J. W. Beeman, A. Javey, J. W. Ager, Y. Liu, F. M. Toma, and I. D. Sharp, *Nat. Commun.* **7**, 12446 (2016).
- ¹⁴⁰J.-H. Yang, W.-J. Yin, J.-S. Park, and S.-H. Wei, *J. Mater. Chem. A* **4**, 13105 (2016).
- ¹⁴¹Y. Lin, B. Chen, Y. Fang, J. Zhao, C. Bao, Z. Yu, Y. Deng, P. N. Rudd, Y. Yan, Y. Yuan, and J. Huang, *Nat. Commun.* **9**, 4981 (2018).
- ¹⁴²J. Xing, Q. Wang, Q. Dong, Y. Yuan, Y. Fang, and J. Huang, *Phys. Chem. Chem. Phys.* **18**, 30484 (2016).
- ¹⁴³D. J. Slotcavage, H. I. Karunadasa, and M. D. J. A. E. L. McGehee, *ACS Energy Lett.* **1**, 1199 (2016).
- ¹⁴⁴H. Zhang, X. Fu, Y. Tang, H. Wang, C. Zhang, W. W. Yu, X. Wang, Y. Zhang, and M. Xiao, *Nat. Commun.* **10**, 1088 (2019).
- ¹⁴⁵E. T. Hoke, D. J. Slotcavage, E. R. Dohner, A. R. Bowring, H. I. Karunadasa, and M. D. McGehee, *Chem. Sci.* **6**, 613 (2015).
- ¹⁴⁶V. M. Goldschmidt, *Naturwissenschaften* **14**, 477 (1926).
- ¹⁴⁷Z. Li, M. Yang, J.-S. Park, S.-H. Wei, J. J. Berry, and K. Zhu, *Chem. Mater.* **28**, 284 (2016).
- ¹⁴⁸A. Dualeh, N. Tétreault, T. Moehl, P. Gao, M. K. Nazeeruddin, and M. Grätzel, *Adv. Funct. Mater.* **24**, 3250 (2014).
- ¹⁴⁹Y. Liu, Z. Yang, D. Cui, X. Ren, J. Sun, X. Liu, J. Zhang, Q. Wei, H. Fan, F. Yu, X. Zhang, C. Zhao, and S. Liu, *Adv. Mater.* **27**, 5176 (2015).
- ¹⁵⁰Y. Dang, Y. Zhou, X. Liu, D. Ju, S. Xia, H. Xia, and X. Tao, *Angew. Chem. Int. Ed.* **55**, 3447 (2016).
- ¹⁵¹L. Wang, H. Zhou, J. Hu, B. Huang, M. Sun, B. Dong, G. Zheng, Y. Huang, Y. Chen, L. Li, Z. Xu, N. Li, Z. Liu, Q. Chen, L.-D. Sun, and C.-H. Yan, *Science* **363**, 265 (2019).
- ¹⁵²N. Li, S. Tao, Y. Chen, X. Niu, C. K. Onwudinanti, C. Hu, Z. Qiu, Z. Xu, G. Zheng, L. Wang, Y. Zhang, L. Li, H. Liu, Y. Lun, J. Hong, X. Wang, Y. Liu, H. Xie, Y. Gao, Y. Bai, S. Yang, G. Brocks, Q. Chen, and H. Zhou, *Nat. Energy* **4**, 408 (2019).
- ¹⁵³S. Bai, P. Da, C. Li, Z. Wang, Z. Yuan, F. Fu, M. Kawecki, X. Liu, N. Sakai, J. T.-W. Wang, S. Huettnner, S. Buecheler, M. Fahlman, F. Gao, and H. J. Snaith, *Nature* **571**, 245 (2019).
- ¹⁵⁴X. Zheng, Y. Hou, C. Bao, J. Yin, F. Yuan, Z. Huang, K. Song, J. Liu, J. Troughton, N. Gasparini, C. Zhou, Y. Lin, D.-J. Xue, B. Chen, A. K. Johnston, N. Wei, M. N. Hedhili, M. Wei, A. Y. Alsalloum, P. Maity, B. Turedi, C. Yang, D. Baran, T. D. Anthopoulos, Y. Han, Z.-H. Lu, O. F. Mohammed, F. Gao, E. H. Sargent, and O. M. Bakr, *Nat. Energy* **5**, 131 (2020).
- ¹⁵⁵M. Li, W. W. Zuo, Q. Wang, K. L. Wang, M. P. Zhuo, H. Köbler, C. E. Halbig, S. Eigler, Y. G. Yang, X. Y. Gao, Z. K. Wang, Y. Li, and A. Abate, *Adv. Energy Mater.* **10**, 1902653 (2019).
- ¹⁵⁶T. Niu, J. Lu, R. Munir, J. Li, D. Barrit, X. Zhang, H. Hu, Z. Yang, A. Amassian, K. Zhao, and S. F. Liu, *Adv. Mater.* **30**, 1706576 (2018).
- ¹⁵⁷Y. Cho, A. M. Soufiani, J. S. Yun, J. Kim, D. S. Lee, J. Seidel, X. Deng, M. A. Green, S. Huang, and A. W. Y. Ho-Baillie, *Adv. Energy Mater.* **8**, 1703392 (2018).
- ¹⁵⁸S. Yang, S. Chen, E. Mosconi, Y. Fang, X. Xiao, C. Wang, Y. Zhou, Z. Yu, J. Zhao, Y. Gao, F. De Angelis, and J. Huang, *Science* **365**, 473 (2019).
- ¹⁵⁹Y. Wang, T. Wu, J. Barbaud, W. Kong, D. Cui, H. Chen, X. Yang, and L. Han, *Science* **365**, 687 (2019).
- ¹⁶⁰R. Wang, J. Xue, K.-L. Wang, Z.-K. Wang, Y. Luo, D. Fenning, G. Xu, S. Nuryyeva, T. Huang, Y. Zhao, J. L. Yang, J. Zhu, M. Wang, S. Tan, I. Yavuz, K. N. Houk, and Y. Yang, *Science* **366**, 1509 (2019).